TAMPEREEN TEKNILLINEN YLIOPISTO
TAMPERE UNIVERSITY OF TECHNOLOGY

TIMO HUUSARI

ANALOG RF CANCELLATION OF SELF INTERFERENCE IN FULL-DUPLEX TRANSCEIVERS

Master's Thesis

The examiner and topic of the thesis were approved by the Council of the Faculty of Computing and Electrical Engineering on 13 August 2014.

ABSTRACT

Master's Degree Program in Electrical Engineering
TIMO HUUSARI: Analog RF Cancellation of Self Interference in Full-Duplex Transceivers
Tampere University of Technology
May 2015
Master of Science Thesis, 59 pages, 2 Appendix pages
Major: Wireless Communications
Examiners: Professor Mikko Valkama, University Lecturer Olli-Pekka Lundén

Keywords: Analog, Cancellation, Full-duplex, RF, Tracking

Current wireless radio technologies use either *frequency domain duplexing* (FDD) or *time domain duplexing* (TDD) to provide transmission and reception. The former uses two separate channels whereas the latter alternates between *transmission* (TX) and *reception* (RX). In-band full-duplex operation uses only one channel and provides bi-directional communication and therefore doubles the spectral efficiency. This is the main benefit of in-band full-duplex operation.

The main challenge in this operation is the *self-interference* (SI) which is due to own TX-signal leaking to the receiver. Without any cancellation this interference signal masks all the desired RX-signals and in-band full-duplex operation is not possible. The cancellation can be done using a simple approach of subtracting own TX-signal from the receiver. This needs to be done both in analog domain and in digital domain. The shared cancellation protects the sensitive receiver and relieves the requirements for *analog to digital* (AD)-converters. The required amount of cancellation is unrealistic to be achieved by using only analog or digital cancellation.

In this thesis, a novel analog active canceller device is designed and implemented. It is based on a research done in Intel Wireless labs[1] with whom *Tampere University of Technology* (TUT) has currently collaboration. The device is capable of canceling wideband signals by adjusting the phase and amplitude. It has a self-adaptive control which can converge to the optimum cancellation and track sudden changes in the SI-signal. A fully analog dual-tap canceller was implemented at TUT premises.

The measurement results verify the theory of operation. The canceller can track the changes quickly and provides total analog cancellation 46 dB to 56 dB depending on the antenna interference. Out of this, 24 dB to 34 dB is provided by the canceller. This is obtained when using 20 MHz wide *long term evolution* (LTE) waveform with approximately 20 dBm TX-power. When measured in collaboration with Aalto University using a combined setup, the system was able to cancel 23.5 dBm signal down to the receivers noise floor. These results compare well against other results presented in academia.

This thesis shows that in-band full-duplex operation is feasible. It is still in very early stages and there remains a vast amount of work and optimization still to be done.

[1] Y.-S. Choi and H. Shirani-Mehr, "Simultaneous transmission and reception: Algorithm, design and system level performance," *IEEE Transactions on Wireless Communications*, vol. 12, no. 12, pp. 5992–6010, Dec. 2013.

TIIVISTELMÄ

TIMO HUUSARI: ITSEHÄIRIÖN ANALOGINEN RF-KUMOAMINEN
Tampereen teknillinen yliopisto
Diplomityö, 59 sivua, 2 liitesivua
Sähkötekniikan diplomi-insinöörin tutkinto-ohjelma
Toukokuu 2015
Pääaine: Wireless Communications
Tarkastajat: professori Mikko Valkama, yliopistonlehtori Olli-Pekka Lundén

Avainsanat: analoginen, full-duplex, kumoaminen, RF

Nykyiset langattomat järjestelmät käyttävät joko aika- tai taajuusjakoista dupleksointia mahdollistaakseen lähetyksen ja vastaanoton. Aikajakoisessa dupleksoinnissa vaihdellaan nopeasti lähetyksen ja vastaanoton välillä käyttäen yhtä kanavaa kun taas taajuusjakoisessa käytetään eri kanavia lähetykseen ja vastaanottoon. Full-duplex -toiminnassa käytetään yhtä kanavaa yhtäaikaa lähetykseen ja vastaanottoon. Verrattuna edellämainittuun se kaksinkertaistaa spektrin käytön tehokkuuden. Tämä on suurin hyöty, joka saadaan full-duplex -toiminnasta

Suurin haaste full-duplex -toiminnassa on niin sanottu itsehäiriö, joka on vastaanottimeen kytkeytyvä oma lähetyssignaali. Ilman mitään kumoamista tämä häiriö peittää kaikki halutut signaalit allensa eikä full-duplex -toiminta ole mahdollista. Kumoaminen voidaan toteuttaa yksinkertaisesti vähentämällä oma lähetys vastaanottimesta. Tämä täytyy tehdä sekä analogisesti että digitaalisesti. Jaettu kumoaminen suojaa vastaanottimen herkkiä komponentteja sekä keventää analogia-digitaalimuuntimen dynamiikkavaatimuksia. Tarvittava kumoamismäärä on epärealistisen suuri saavutettavaksi pelkästään analogisella tai digitaalisella kumoamisella.

Tässä diplomityössä on kehitetty ja rakennettu uudentyyppinen aktiivinen kumoamislaite. Se perustuu Intel Wireless -laboratorioissa tehtyyn tutkimukseen[1] nykyisen tutkimusyhteistyöprojektin puitteissa. Laite voi kumota laajoja signaaleita säätäen amplitudia ja vaihetta. Siinä on itsestään säätyvä ohjaus, joka pystyy löytämään optimaalisen kumoamispisteen sekä seuraamaan itsehäiriösignaalissa tapahtuvia äkillisiä muutoksia. Konseptista rakennettiin kaksitappinen täysin analoginen kumoamislaite Tampereen teknillisen yliopiston tiloissa.

Saadut mittatulokset vahvistavat teoreettisen analyysin. Kumoamislaite pystyy seuraamaan muutoksia nopeasti ja kumoaa automaattisäädöllä kokonaisuudessaan 46-56 dB, jossa laitteen kumoamisosuus on 24-34 dB riippuen antenniin kohdistuvasta häirinnästä. Tämä tulos on saatu käyttäen 20 MHz laajaa signaalia noin 20 dBm lähetysteholla. Mitattaessa yhteistyössä Aalto-yliopiston kanssa kokonaisjärjestelmä pystyi kumoamaan 23,5 dBm tehoisen signaalin vastaanottimen kohinalattiaan asti. Nämä tulokset kestävät hyvin vertailun muiden tiedemaailmassa julkaistujen tulosten kanssa.

Tämä diplomityö osoittaa, että full-duplex -toiminta on mahdollista. Nämä ovat vasta ensi askeleita ja työtä ja optimointia on vielä paljon jäljellä.

[1] Y.-S. Choi and H. Shirani-Mehr, "Simultaneous transmission and reception: Algorithm, design and system level performance," *IEEE Transactions on Wireless Communications*, vol. 12, no. 12, pp. 5992–6010, Dec. 2013.

PREFACE

This Master's thesis has been done in Tampere University of Technology during 2014-2015. The actual writing process was done at the end when all the measurement results were already acquired. It is a nice feeling to be writing this page.

I think I managed to find from the beginning the right way to this kind of thesis. The practical work and measurements were conducted first and in the end the actual thesis was written. I hope this thesis could give you a good overview of full-duplex operation, its benefits and what it is like to design a board. I learned a lot during the process and I hope that you could learn from my experiences as well.

Many people deserves my thanks starting from my colleagues and professor Mikko Valkama. Mikko invited me to join the full-duplex research group and that's how it all got started. Many tips&tricks were shared between colleagues, thank you! Thank you Janis Werner and Petteri Liikkanen for the high quality photos. Many thanks to Yang-Seok Choi and the Intel team, with whom I have had many fruitful discussions. We also had the opportunity of participating Mobile World Congress with them and demonstrated the canceler in action with Dani Korpi and Mikko Valkama.

I want to thank you also Olli-Pekka Lundén for your valuable comments when reviewing my thesis. You pointed out many important things that helped me to polish this thesis.

A special thanks to Petteri Liikkanen with whom the board was designed and canceler built. Together we shared all the ups and downs throughout the project. When making the very initial measurements we agreed to be satisfied with more than 30 dB active cancellation. In the end, that target was reached.

Finally, I want to thank my family for all the support and intercessions. Those have supported not only during this thesis project but also throughout my studies. Thank you!

Tampere May 19, 2015
Timo Huusari

Tekniikankatu 10 C 149
33720
TAMPERE
+358405372096

"Trust in the LORD with all your heart and lean not on your own understanding; in all your ways submit to him, and he will make your paths straight."

Proverbs 3:5-6 (NIV)

CONTENTS

LIST OF FIGURES

LIST OF SYMBOLS AND ABBREVIATIONS

ABBREVIATIONS

3^{rd} IMD	**3^{rd} order intermodulation distortion**
ADS	**Advanced Design System**, an extensive RF CAD software
AC	**alternating current**
ADC	**analog-to-digital converter**
AD	**analog to digital**
BB	**baseband**, contrary to RF baseband means operating with signals centered at DC
CSMA	**carrier sense multiple access**
dB	**decibel**, unit of ratio. For voltages it is defined as $20\log_{10}(V_1/V_2)$ and for powers $10\log_{10}(P_1/P_2)$
DAC	**digital-to-analog converter**
DC	**direct current**
EIRP	**effective isotropic radiated power**, power required for an isotropic antenna to radiate
FIR	**finite impulse response**
FDD	**frequency domain duplexing**
HD	**high definition**
ISM	**industrial, scientific, medical**, free to use bandwidth
IQ	**in-phase and quadrature**, a representation of complex baseband signals such that I is the real part and Q is the imaginary part.
IIP_3	**input referred 3^{rd} IMD intercept point**
LMS	**least mean squares**, an adaptive filter algorithm
LO	**local oscillator**
LTE	**long term evolution**, a general term describing post 3G network technologies [1]
LPF	**low pass filter**
LNA	**low noise amplifier**
NF	**noise figure**
PA	**power amplifier**
PCB	**printed circuit board**
RF	**radio frequency**
RX	**reception**
RLS	**recursive least squares**, an adaptive filter algorithm
RBW	**resolution bandwidth**

[1] Geßner, C., *Long Term Evolution — A concise introduction to LTE and its measurement requirements,* Munich, Germany: Rohde & Schwarz, 2011

R&S	**Rohde & Schwarz**, an electrical test and measurement device manufacturer
RMS	**root, mean, square**, value computed from ac-signal that can be compared directly with DC-signal in terms of power.
SI	**self-interference**, undesired tx-signal leaking one way or another to the rx-chain
SoI	**signal of interest**
SNR	**signal-to-noise ratio**
SMA	**sub miniature "type A"**, a common connector type for rf-devices and measurement equipment
SMD	**surface mount device**, contrary to through hole devices these devices populate only one side of the PCB and are available in miniature sizes
TUT	**Tampere University of Technology**
TDD	**time domain duplexing**
TX	**transmission**
VGA	**variable gain amplifier**
VNA	**vector network analyzer**, a device capable of measuring accurate phase and amplitude response of a device under test
VST	**vector signal transceiver**, a device capable of measuring accurate amplitude and phase response.
WLAN	**wireless local area network**

SYMBOLS

δ	dissipation factor
Δ_{τ_k}	tap delay difference
ε_{r}	relative permittivity
μ	step size

TERMS

balanced	balanced or differential signaling means that the signals are not referred to ground. The information is stored in the difference of two signals. This makes the signal very robust against common mode interference.
bias	bias is a operating setpoint for a transistor or generally for an active device such as an amplifier.
Bluetooth	Bluetooth is a standard for short range wireless communications.

characteristic impedance	characteristic impedance is the ratio of traveling voltage wave to traveling current wave in a transmission line. [1]
scattering parameter	A method of characterizing an arbitrary n-port network using reflected and transmitted signals, i.e. scattering parameters.
schmitt-trigger	a type of comparator structure. Comparator is device changing its output from minimum to maximum (or vice versa) when the threshold is crossed.
Smith Chart	a special type of a chart that represents the right half of the complex plane in a circle.
tap	tap is a an element of FIR-filter.
via	via is a metal plated hole connecting layers of a PCB.
weight	weight is the current control value of a tap.
WiFi	WiFi or Wireless Fidelity is a standard for wireless communications, especially used to deploy WLAN.

[1] D. M. Pozar, *Microwave Engineering*, page 50, 4th ed. USA: Wiley, 2012.

1. INTRODUCTION

In our everyday life smart phones, tablets and other wireless communications play a significant role. We consult our e-mails, check news and weather forecasts, play online games and even stream *high definition* (HD)-video to our pocket devices. All this has happened in relatively short period of time and the progress in wireless communications data throughput has evolved astonishingly fast. However, there are theoretically derived upper limits for amounts of information that can be transferred using certain amounts of resources [1]. Current modulation technologies are soon reaching these limits. Significant growth potential for capacity and speed must be sought elsewhere.

Currently, in order to transmit and receive, two common approaches are used. Those are *time domain duplexing* (TDD) and *frequency domain duplexing* (FDD). Both of these techniques allow either transmission or reception at a time on a channel. The capacity can be doubled by so called in-band full-duplex meaning simultaneous transmission and reception on the same channel. Such a simple change doubles the spectral efficiency as all the channels can be used at the same time for transmission and reception. This is a huge advantage over TDD and FDD. The operators and industry are thus very interested in this technology. Moreover, it is a very low level change and it can be applied to any kind of wireless standards. Figure 1.1 compares the essential characteristics of these three duplexing methods.

The idea of transmitting and receiving at the same time on the same channel is nothing new. There are for example full-duplex Ethernet connections which can be used in wired networks. The simultaneous transmission and reception can indeed

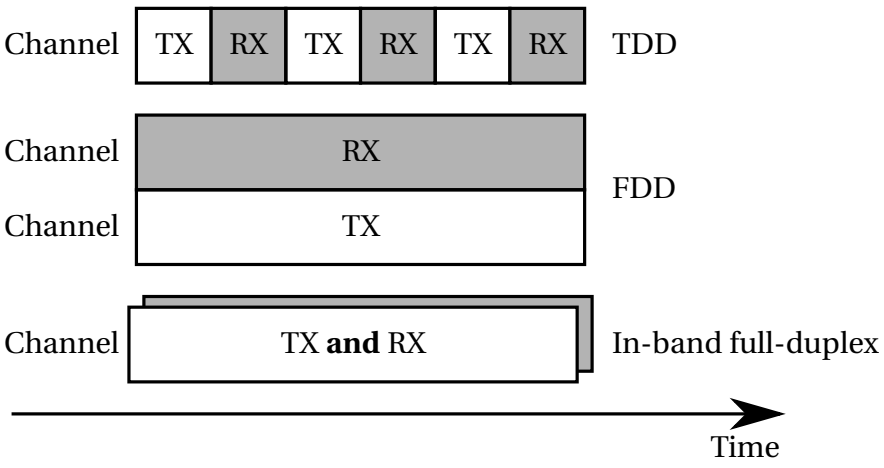

Figure 1.1. *In-band full-duplex operation compared to classical TDD and FDD.*

be achieved easily, one simply wires another pair of cables for transmission to another direction. However, when using wireless communications one cannot separate the transmission and reception as the radio waves share the same medium, the air. This leads to the main reason why wireless in-band full-duplex has been previously rejected. It has been thought to be impossible. The own *transmission* (TX) signal will appear—more or less attenuated—at the own receiver causing an enormous *self-interference* (SI). This SI dominates the receiver and all the desired signals are absolutely buried under this strong signal. Without any attenuation of this SI in-band full-duplex operation is obviously not possible.

Fortunately, the transmit signal eventually turning into SI is perfectly known beforehand. This allows one to simply subtract the own transmission from the receiver leaving the desired signals intact. As simple as it sounds, this is the actual approach to cancel out the SI. More thorough examination reveals that the SI signal is actually not exactly the same than the original TX signal. In order to achieve cancellation this transmit signal needs to be thus adjusted to match with the SI signal. It turns out that achieving good levels of SI-cancellation requires very precise matching between these two signals. This is the main challenge of the SI-cancellation.

In spite of the required cancellation performance requirements, the advantages of the in-band full-duplex operation has motivated recently many research groups and industry to pursue a practical realization of full-duplex transceiver. Active research has been done around the globe and one of the most well-known research groups was based at Stanford University [2, 3, 4]. That has already led to a start-up company called Kumu Networks [5]. Industry is active in the research as well but naturally they are not as open as academia to present current results.

The aim of this master's thesis is to develop and build an analog active *radio frequency* (RF)-canceller taking care of the analog domain cancellation. It is a part of a current research project at the department of Electronics and Telecommunications engineering at *Tampere University of Technology* (TUT). Author's contribution has been taking care of the practical realization and RF-related matters as well as conducting practical measurements. During the process two revisions of canceller boards were made proving the concept to be functional. Many measurements were conducted and results were published in collaboration with Aalto University and Intel Wireless labs [6, 7]. Lastly, collaborating with Intel Wireless labs the combined analog and digital cancellation was demonstrated at Mobile World Congress 2015 in Barcelona, see Figure 1.2.

The thesis is organized as follows. In the next chapter, the background theory for in-band full-duplex operation is revised and the problem itself is set from the background theory. A brief presentation of other research groups' work related to full-duplex is presented as well. Moving on to the third chapter, the theory of operation, design and implementation of the canceler device are presented. Chapter four is

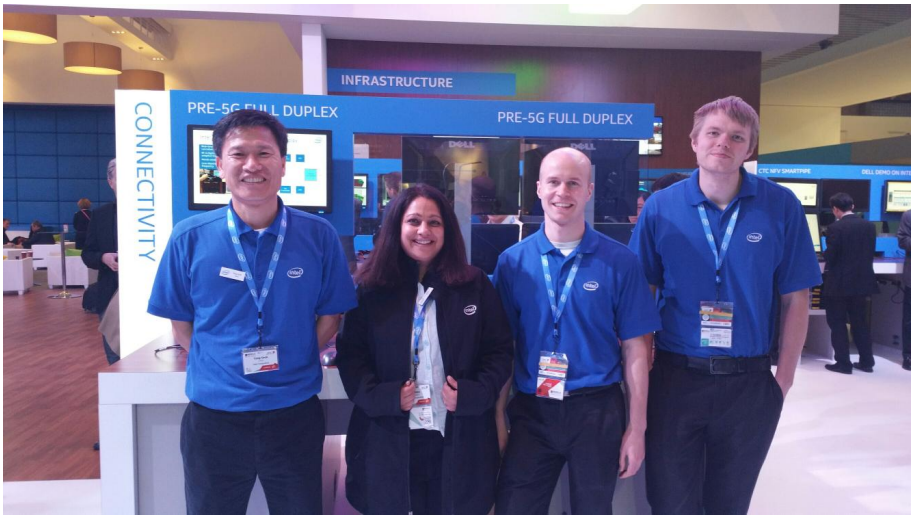

Figure 1.2. *Demonstrating in-band full-duplex cancellation at Mobile World Congress 2015. From left to right: Yang-Seok Choi (Intel), Shilpa Talwar (Intel), Timo Huusari (author, TUT) and Dani Korpi (TUT). Absent from this picture Mikko Valkama (TUT). Figure used with permission from Intel.*

dedicated to measurement results and their analysis. At the end a comparison with other results from academia and industry is done. Lastly, chapter five concludes this thesis.

For the nomenclature, in-band full-duplex is shortened to full-duplex. Mathematical symbols are presented in italics style. The terms and abbreviations occurring first time are typeset in italics.

2. THEORETICAL BACKGROUND AND PROBLEM SETTING

In this chapter the background theory for full-duplex operation is presented briefly. As it will be seen the full-duplex operation cannot be simply separated to be an antenna, RF nor *baseband* (BB) related challenge, all of these must be introduced and taken into account. Alongside the introductions to various parts concerning full-duplex operation the benefits and motivation for it are discussed. Finally, current research activity and other approaches are presented at the end of this chapter.

2.1 Direct conversion transceiver

The term radio can be used to describe a device that is capable of receiving an electromagnetic signal or transmitting it. To be more precise, most of the radios, such as the colloquial language radio is a receiver. On the other hand, the radio of the mobile phone is capable of receiving and transmitting signals, i.e. it has a receiver and transmitter. This is called a transceiver.

There are many types of receiver and transmitter structures developed mostly during the 20th century. Direct conversion transceiver is a structure where BB signal is converted directly to RF-frequencies. This structure has become commonly used in current mobile transceiver architectures and hence it is used also in this full-duplex canceler project. The essential parts of it are depicted in Figure 2.1.

The TX bits come from coder and are then converted into analog signal using a *digital-to-analog converter* (DAC). *In-phase and quadrature* (IQ) is the representation

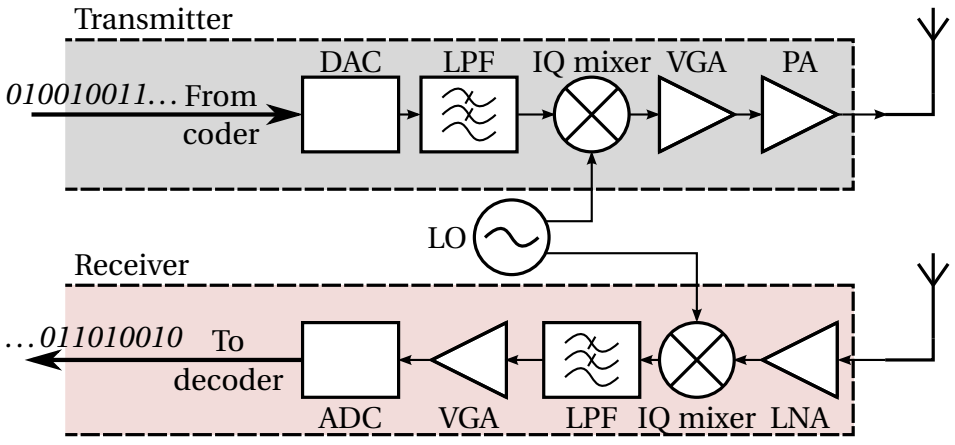

Figure 2.1. *High level block diagram of direct conversion transceiver. [8, p.101]*

of the complex BB data. Then the signal is low-pass filtered, mixed with *local oscillator* (LO) and amplified with *variable gain amplifier* (VGA) and *power amplifier* (PA).

The receiving side consists of a *low noise amplifier* (LNA), downconverting IQ mixer, low pass filtering, a VGA and an *analog-to-digital converter* (ADC). The VGA controls the received signal strength such that the maximum dynamic range of the ADC can be utilized regardless of variations in the received power.

2.2 Motivation for the full-duplex

Duplex stands for a system that is capable of transmitting two signals simultaneously to opposite directions [9]. Full-duplex is a synonym for duplex. Half-duplex can transmit only to one direction at a time. Common full duplex method is FDD and half duplex method TDD. In FDD up-link and down-link transmissions are done using two different frequency channels and in TDD the system alternates between transmission and reception using time slots [10, p.31]. In this thesis full-duplex term is used for transmission taking in place at the same frequency at the same time, i.e. in-band full-duplex.

In-band full-duplex wireless communications have been an active area of research recently. It is a very fundamental change in communications and commonly it has been taken as granted that it is not possible to transmit and receive simultaneously [2].

Some of the advantages are obvious such as theoretically doubling the capacity due to the full-duplex operation [3, 11]. In practice, there will be some overhead but nevertheless already using demonstration devices an increase of 87 % has been achieved [3].

Another very strong benefit is the reduction of frequency requirements. Currently many systems use FDD techniques which require a certain amount bandwidth for transmission and the same amount of bandwidth for reception. It is obvious that using full-duplex only one band is sufficient for both transmission and reception and thus the expensive and scarce frequency bands can be used more efficiently. In practice this would allow for example two operators to operate using same frequency resources which were needed previously for only one operator using half-duplex operation.[3]

Full-duplex advantages go beyond physical layer improvements [2, 11]. Using full-duplex operation, the common hidden node problem can be almost completely eliminated. Hidden node problem is common in *carrier sense multiple access* (CSMA) networks, e.g. *WiFi*-networks, where protocol has been set up such that in order to transmit, the sender must check that the channel is free. However, this does not guarantee a collision free transmission as two senders from opposite edges of the network transmitting to the middle of the network cannot receive each other's signals and thus they interpret the channel to be free all the time. The access point in the middle cannot receive these signals as they collide. Full-duplex operation allows the

access point in the middle to transmit a channel-in-use signal while receiving. This makes others to wait until the channel is free.[2, 11]

From time to time there is a need for relay stations for example to increase coverage to certain direction. A relay station simply amplifies and forwards whatever it receives. In half-duplex operation it must receive the whole message before transmitting it. This causes a delay which is proportional to number of hops[1] in the relay chain. Using full-duplex transmission the relay station can start forwarding the message while receiving it. This reduces the end to end delay considerably. [2, 11, 12]

Operation in full-duplex would be advantageous for cognitive radio systems. Cognitive radio systems take advantage of the fact that although a certain band is allocated to dedicated usage and users, there will be moments when the channel is silent. To increase the efficiency of spectral usage another user could transmit their own data during these silent moments and quickly release the band for the dedicated user when a transmission is sensed. Full-duplex systems are a natural choice for cognitive radios as it makes possible to monitor channel while transmitting and thus push the cognitive radios one step onward.[2, 11] All in all, full-duplex is a fundamental change in wireless communications providing many advantages.

2.3 Full-duplex methods

Full-duplex operation can be achieved using for example two antennas; one for TX and one for *reception* (RX). In this case the separation of the antennas provides intrinsic isolation between the TX and RX chains. Additionally a more complex antenna system can be used to improve this isolation for example by creating a suitable transmit null at the point of the receiving antenna. Depending on the antenna radiation requirements more isolation can be achieved using directive antennas. One example is a full-duplex relay antenna designed in Aalto-University providing more than 50 dB of isolation between TX and RX chains [7].

Full-duplex operation is possible also using a single antenna. In this case a circulator is needed to achieve full-duplex operation. Alternatively, an electrical balance network can be used as well. Figure 2.2 depicts these two commonly used full-duplex system architectures.

The advantage of multi antenna setup is the lower cost as affordable antennas can be manufactured using printed circuit technology. However, the extra antennas can be problematic as antennas affect each other when they are closely spaced. Depending of the required minimum isolation a certain amount of separation is required. Combining these two requirements yields an increased minimum size for the device with respect to half-duplex counterpart.

[1] A hop is the link between two stations.

Circulator setups do not require any extra antennas, but circulators are more expensive and passive ones cannot be miniaturized. On the other hand a circulator can be made electronic at the expense of adding noise sources and lowering maximum power handling capacity. Circulators too will increase the size of the device but only due to size of the circulator itself. When aiming for mobile devices the requirement for doubling the amount of antennas might become impossible to achieve due to the unwanted antenna interaction using closely spaced antennas. This challenge is pronounced with MIMO antenna systems. The focus of this thesis is on to develop an analog RF-cancellation device especially for circulator based operation.

2.4 Causes of the self-interference

Let us briefly examine the main characteristics of a circulator regarding full-duplex operation. A circulator is a three port device which steers signal through its ports such that the signal comes in from one port and then exits the circulator from the second port depending on the sense of rotation (i.e. clockwise or counter clockwise). In an ideal case the signal cannot propagate to the opposite direction and the third port is thus isolated. This principle applies to all ports of the circulator and this property makes it possible to have full-duplex operation using only one antenna [13].

Real world circulators can either be active or passive devices, the latter ones being more common. A permanent magnet inside the circulator provides bias magnetic field. The magnet magnet makes the sense of rotation fixed and the device completely passive. The theory of operation of the passive circulator can be understood as a resonance structure which creates a destructive interference at the third port. Hence the aforementioned operation is achieved. Depending on the size of the circulator typical values for isolation (signal leaking to the undesired direction) is in the order of 20 dB to 30 dB [14]. In theory, the circulator isolation is directly proportional to the input return loss of its ports [13, p.488]. The attenuation in the desired direction is small and usually less than half of a decibel. Circulator is a bandwidth limited device but wide bandwidth operation can be attained at the expense of worse isolation. Being a passive device, the size is ultimately dictated by the wavelength of the operating frequency [13].

(a) *Dual antenna based architecture.* ***(b)*** *Circulator based architecture.*

Figure 2.2. *Typical full-duplex architectures.*

The above mentioned isolation directly translates to the amount of SI caused by the circulator. However, isolation can be traded off for bandwidth.

The second strong source of SI is the power reflected by antenna. Reflection coefficient Γ is a measure of the amplitude and phase of the reflected signal. It can be computed using impedances [13, p.1] as

$$\Gamma = \frac{Z_L - Z_0}{Z_L - Z_0} \tag{2.1}$$

where Z_L is the load impedance and Z_0 is the reference impedance of the system, e.g. transmission line. Return loss L_{retn} is a measure of how much the reflected power is attenuated with respect to the originally incident power and it is computed from Γ as

$$L_{\text{retn}} = -20 \log |\Gamma|. \tag{2.2}$$

In jargon, return loss is called matching. Typically the systems work using 50 Ω as the reference impedance [15, p.59,p.175]. Perfectly matched input makes the device to accept all the supplied power whereas a mismatch will cause part of this power to be reflected back to the transmission line. Also the antenna needs to be designed and matched such that at desired frequency (band) of operation the input impedance equals to Z_0. However, in reality some of the power always reflects. A de-facto value for antenna matching is 10 dB as better matching does not increase transmitted power significantly any more [15, p.177]. With 10 dB return loss 90 % of power is transmitted. However, for the full-duplex case increasing the antenna matching translates directly to reduced amount of SI. Therefore, for full-duplex operation high return loss is desired. Return loss values better than 20 dB are seldom obtained and the reflection from antenna contributes the most to the overall SI.

Figure 2.3 depicts the main SI sources of a circulator system. Furthermore, depending on the surrounding objects of the antenna, some reflections can be strong enough to cause unwanted SI into the RX chain.

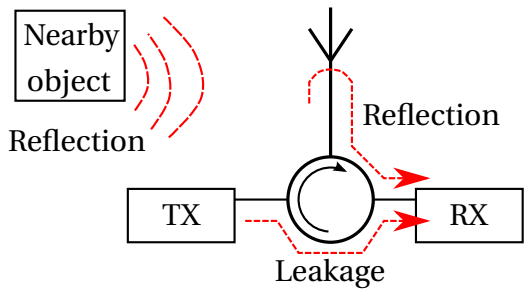

Figure 2.3. *Main sources of SI in circulator setups.*

2.5 Measured SI characteristics of circulator and antenna

The design process started by characterizing typical circular and antenna SI properties. These included the delays of the components as well as the amplitudes of the components. The amplitude of the SI components was conveniently measured using a *vector network analyzer* (VNA).

Circulators are available in different form factors. Smaller ones can be made thinner but the footprint stays the same because of the wavelengths. In this project only coaxial circulators were used. Those are in their own small case with coaxial connectors *sub miniature "type A"* (SMA) which allows convenient working and connection between different devices. The tested circulators are MESL SG 10522, JQL Electronics JCC2300T2500S10 and JCC2300T2500S6. Surface mount circulators provide similar performance with lower maximum allowed power levels [14].

Table 2.1 presents measured values along with data sheet values for two different types of a circulator. Appendix 1 lists complete measurement data of the MESL SGL 10522 circulator.

The measured values and data sheet ones are consistent. The peak isolation is better than the datasheet value. As the circulator is a three port device, three measurements had to be done to fully characterize the circulator. The measured data could be conveniently combined using Agilent *Advanced Design System* (ADS) Touchstone Combiner. This resulted a single three port *scattering parameter* file.

Three antennas from *wireless local area network* (WLAN) access point were chosen to be used throughout the project. Those represent typical end-user antennas as the full-duplex could be implemented for the WLAN access points. Figure 2.4 presents return loss measurements for three samples of Cisco AIR-ANT2422DB-R antennas. The antennas have good return losses over the ISM bandwidth and especially antenna 3 has a nearly constant L_{retn} of 15 dB. For cancellation signal creation this is a good property. The effective SI channel model becomes more straightforward as there is no frequency dependent attenuation.

Also shown in Figure 2.4 is the effect of introducing something to the proximity of an antenna. Here a hand was gripped around the antenna and the return loss changes as can be seen. This is because at the proximity of the antenna there are reactive fields

Table 2.1. *Comparison of circulators. Measured values are for the 2.4 GHz* industrial, scientific, medical *(ISM)-band.*

	MESL SGL 10522 (ser. 104)		JCC2300T2500S10	
Parameter	Data sheet	Measured	Data sheet	Measured
Isolation (dB)	23	>24	23	>25
Return loss (dB)	23	>25	20.8	>24.5
Insertion loss (dB)	0.3	<0.15	0.3	<0.25

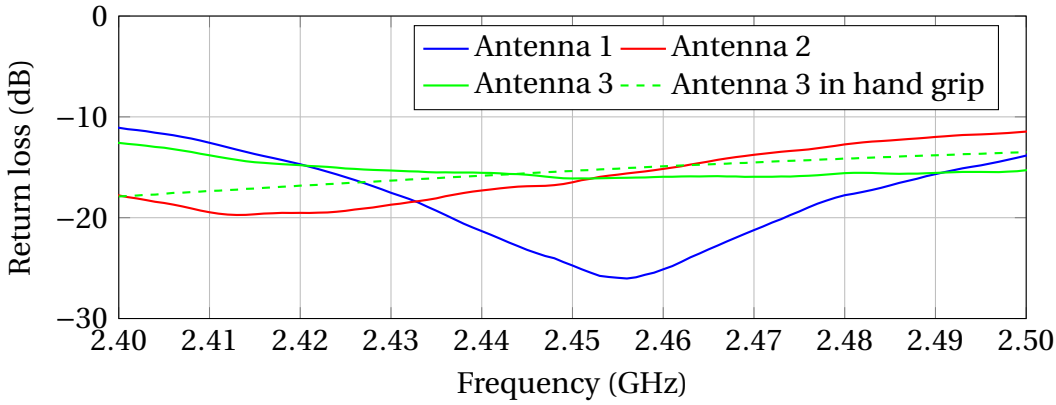

Figure 2.4. *Antenna return loss measurements.*

similar than for example between capacitor plates. For a capacitor the capacitance depends on the material parameters between the plates and similarly for antennas disturbing the reactive fields changes the antenna parameters. That is why return loss changes and this change must be taken into account when designing an RF canceller. This calls for adaptivity in order to track (sudden) changes in the antenna proximity.

As the VNA can measure accurate phase and amplitude responses, it is possible to measure accurate impulse responses as well. The idea is to make measurements in frequency domain with specific frequency step and then using inverse Fourier transform to shift the response to time domain and essentially get an impulse response. Using this method the absolute amplitude values are usually not accurate but the timing is accurate. The measurement accuracy depends on the frequency step size which translates into maximum impulse response time and the highest frequency which translates into the time domain resolution. In other words

$$\text{Time span} = \frac{1}{\Delta f_{\text{step}}} \tag{2.3}$$

$$\text{Time resolution} = \frac{1}{f_{\text{max}}}. \tag{2.4}$$

Note the analogy with sampling an analog time domain signal.[16]

Figure 2.6 presents the impulse response measurement results for a system consisting of a circulator and an antenna, like in Figure 2.3. Figure 2.5 depicts the measurement setup. Impulse response was derived from frequency response data measured using HP-8722D VNA with step-size of 50 MHz and span from 0.05 GHz to 10.05 GHz. These settings provided a maximum measurement time of 20 ns with a resolution of approximately 0.1 ns.

Figure 2.6 reveals many interesting details of the SI. First of all it can be said that it is spread over 6 ns. The zoom in Figure 2.6b reveals that the leakage through the circulator occurs first between 0.25 ns to 0.5 ns. This is because no matter what is

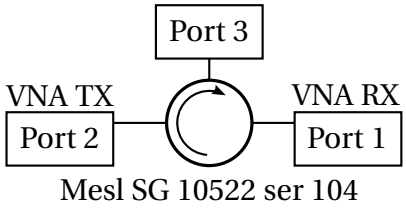

Figure 2.5. *Impulse response measurement setup. Test loads to port 3 were antenna, 50 Ω and it was left open.*

connected to the port 3 the output is the same, hence it must be the leakage. Then between 1 ns to 1.7 ns the signal reflects back from the port 3. Here match yields barely any reflection whereas open port yields very strong reflection as it should. The reflection from antenna comes only at roughly 1 ns later. The used antenna is 15 cm long dipole antenna and forth-back of 30 cm divided by the speed of light yields quite accurately 1 ns which explains the delay. Later there can be seen some multipath reflections at 3.4 ns, 4 ns and 5.5 ns. To conclude, the main SI consist of two strong components due to the circulator leakage and antenna reflection and those are 2 ns apart each other.

2.6 Analog Impairments

In analog signal processing there are always some impairments present. The most common ones are noise and distortion which are analyzed in this section.

Noise power available from a noisy resistor can be computed using [15, p.104]

$$P_N = kT\Delta f, \tag{2.5}$$

where P_N is the noise power in watts, k is the Boltzmann's constant, T is temperature in kelvins and Δf is the specified bandwidth of interest. Thermal noise floor can be computed by simply specifying the amount of power per specified bandwidth. Thus,

$$\text{Noise floor} = \frac{P_N}{\Delta f} = kT \text{ in watts/bandwidth} \tag{2.6}$$

$$= 10 \times \log_{10}\left(\frac{kT \text{ (mW)}}{1 \text{ (mW)}}\right) \text{ in dBm/bandwidth.} \tag{2.7}$$

Substituting the Boltzmann's constant 1.38×10^{-23} J/K, $T = 290$ K and bandwidth of 1 Hz yields –174 dBm/Hz.

Devices also add their own noise to the signal. For example amplifier amplifies input signal and on top of that adds its own noise to the signal. This degradation of *signal-to-noise ratio* (SNR) is called *noise figure* (NF). Noise figure can be determined for all the components, cables, attenuators, mixers, etc. so it is not necessarily related

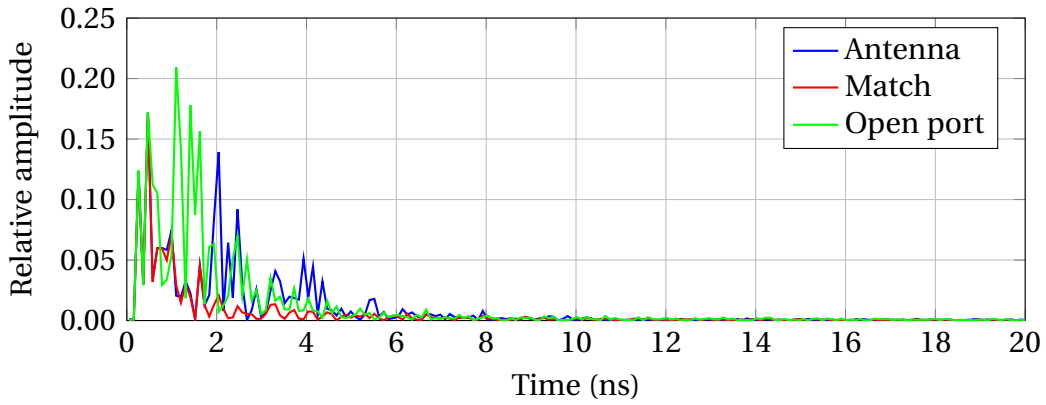

(a) *Full measurement range.*

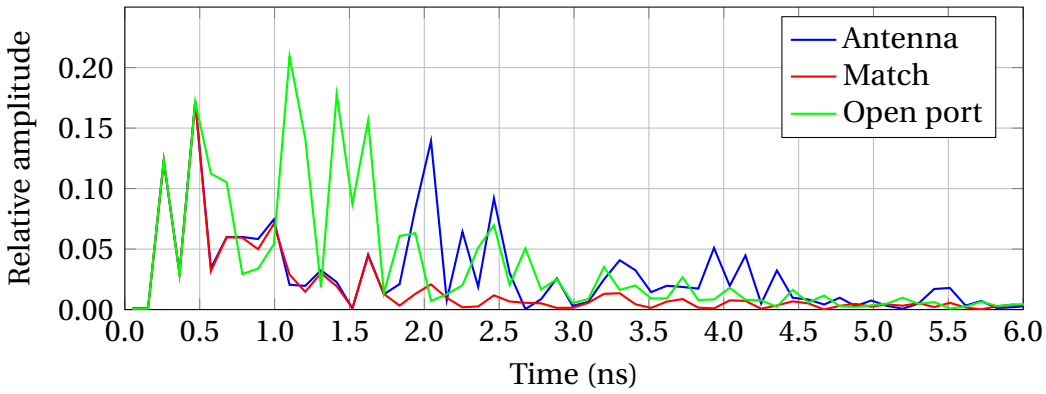

(b) *Zoom in to 6 ns.*

Figure 2.6. *Impulse response of the MESL circulator such that port 3 is connected with antenna, 50 Ω load and left open.*

to amplification. A special type of amplifier is the LNA which is optimized to have a very low noise figure. Noise figure for a system can be determined as a cascade and then it turns out that the NF of the first device or network affects the most to the overall system's NF.[13, p.502-505]

Distortion is commonly measured as harmonic and intermodulation distortion. Harmonic distortion means that the amplifier (or any other device) generates new output signals at multiplies of the input frequency. For example feeding a 1 kHz tone to an amplifier will result tones at 2 kHz, 3 kHz and 4 kHz and so on. The cause for this is often due to the fact that amplifier's supply voltages limit the output voltage swing. This leads to signal clipping and generation of unwanted signal components. The clipping is characterized by 1 dB compression point. This is the input or output power at which the amplifier gain is reduced by 1 dB from linear response due to the compression. Figure 2.7 depicts this phenomenon and the corresponding input and output power points. The components itself such as transistors and diodes may cause distortion. Fortunately harmonic distortion is far away from the signal of interest itself and thus it can be relatively easily filtered out.[13, p.511-516]

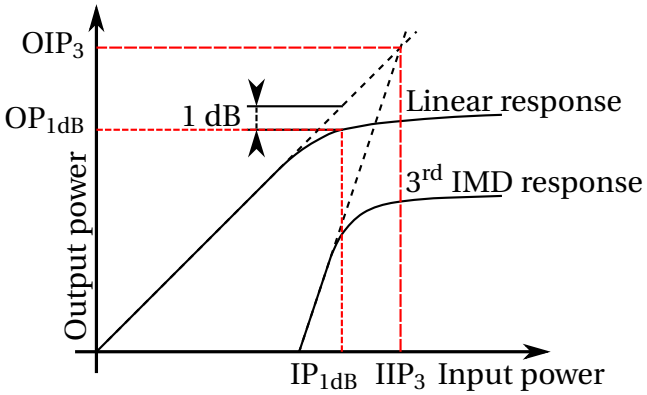

Figure 2.7. *1* decibel *(dB) compression and 3rd intermodulation points depicted. The points are the corners of the red dashed traces.*

Intermodulation on the other hand is far more cumbersome. It is present when the input signal is anything else than a single tone such as two tones, which is a common intermodulation test input. As the name suggests there is internal modulation such that the harmonic components will be mixed with the fundamental ones and with each other. Again many of the results are far away from the fundamental tones but unfortunately couple of components are very close to the fundamental tones. It is difficult if not impossible to filter out these closest components. Assuming two test tones with frequencies f_1 and f_2 the closest components are $2f_2 - f_1$ and $2f_1 - f_2$. These components are so called 3rd order intermodulation components. The figure of merit for intermodulation distortion is commonly measured using intercept points of the linear response and the 3rd intermodulation response. It can be defined for input or output powers similarly as the compression point. Figure 2.7 presents the intermodulation along with the compression.[13, p.511-516]

Here OIP_3 and OP_{1dB} stand for output related interception and compression points, respectively. Similarly IIP_3 and IP_{1dB} stand for the input related values.

2.7 Cancellation

In order to be able to receive simultaneously while transmitting the RX-chain must be free of SI during the transmission. As discussed in the previous section, the circulator and antenna will provide already some attenuation to the self-interference, the author calls this cancellation as intrinsic cancellation (or attenuation). The amount of 20 dB to 30 dB of intrinsic cancellation is not enough for the modern transceiver requirements. Let us justify this with an example of 20 MHz wide WLAN signal.

The maximum TX-power for WLAN in Finland is specified to 100 mW *effective isotropic radiated power* (EIRP) [17, p.11]. This equals 20 dBm. The thermal noise floor is at –174 dBm/Hz which yields –101 dBm/20 MHz.

The receiver always adds own noise on top of the thermal noise and receiver noise figure of 10 dB to 20 dB could be assumed. Hence the SI-power needs to be less than

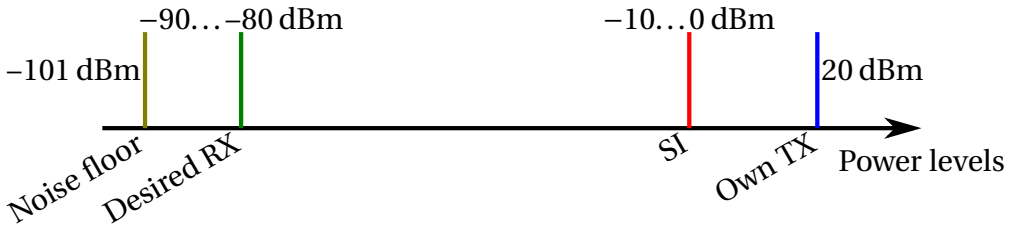

Figure 2.8. *Visualization of power levels.*

some –91 dBm to –81 dBm at the receiver in order not to increase the receiver noise and interference and thus maximize sensitivity in the RX-chain. A total of 80 dB to 90 dB of active cancellation is required. This is an enormous amount of cancellation as 60 dB is already one millionth of the power and 90 dB means one billionth of the power. This is the main challenge in full-duplex radios. Figure 2.8 depicts aforementioned power levels.

The actual cancellation is done by simply subtracting cancellation signal from received signal. This is possible because the SI is ultimately the own transmit signal which is well-known. To subtract a signal is equal to invert the phase and then add signals. The cancellation is thus done by adding an 180°out of phase signal with the received signal and by the wave superposition the SI signal will be canceled.

While this sounds an easy process the challenges are in the details. To get high levels of cancellation the amplitude must be very accurately the same and phase must be very accurately 180°out of phase in order to achieve good cancellation. To demonstrate the requirements Figure 2.9 serves as an example. Using Matlab a sine wave was generated and then the amplitude or the phase of the cancellation signal was varied. Figure 2.9a depicts the achieved cancellation as a function of amplitude scaling of the cancellation signal (perfect phase) and Figure 2.9b the phase difference (perfect amplitude) of the cancellation signal.

It is obvious that cancellations better than 30 dB to 40 dB are very difficult to achieve. The phase is more important than the amplitude as variation in the phase changes strongly the achieved cancellation and can even increase the output power if the phase is more than 60° out of 180°. On top of that here only one parameter was varied but in real life neither the amplitude nor phase cannot be perfect, at least over a longer period.

Analog signal processing impairments, such as noise, ultimately dictate the available phase and amplitude accuracy and thus the required 80 dB to 90 dB of active cancellation is unrealistic. Fortunately in digital domain the processing accuracy can be adjusted by allocating more bits for the data points and processing. The biggest obstacle in full digital SI cancellation is the required enormous dynamic range of the ADC. This is due to the fact that the receiver must acquire the whole SI signal which is high power and at the same time a very low power desired RX signal. For example an 8-bit ADC can sample signals with approximately 48 dB of dynamic range [18, p.3].

Essentially this means that then the SI power can be no more than 48 dB above the receiver noise floor.

One can conclude also that increasing the bits in ADC relieves the SI-power requirements. While this is true the obstacle is the high resolution ADCs which are expensive and consume more power. Hence 24-bit converters cannot be used.

This is why many researchers and current full-duplex architectures propose a combined analog plus digital SI cancellation. The aim is to cancel the signal already in analog domain, i.e. in RF and/or in BB, and then convert the signal into bits and perform digital cancellation. This relieves the amount of bits required for the *analog to digital* (AD)-converter and also protects the receiving input LNA not to have too high input power which would cause distortion or even saturation. To conclude, analog cancellation is indispensable as it protects the input LNA and lessens the AD-converter required resolution. Figure 2.10 depicts these power levels along with minimum required analog cancellation and the AD-converter dynamic range.

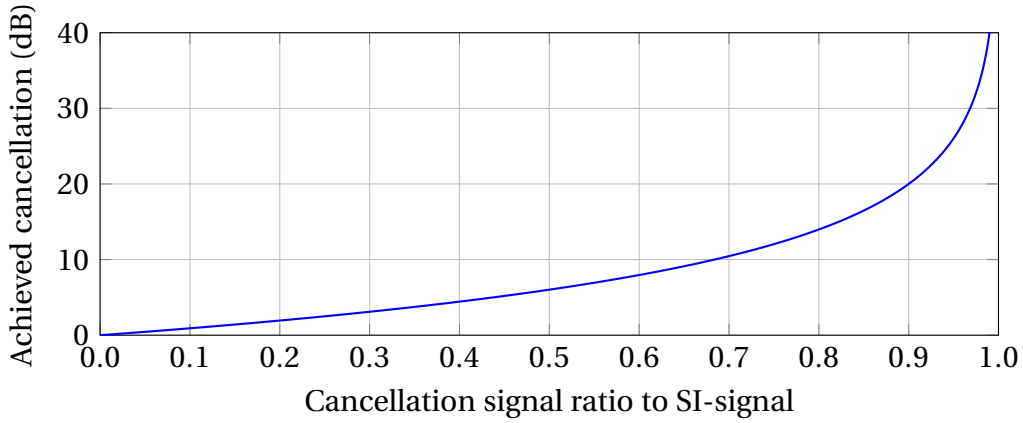

(a) *Effect of cancellation signal amplitude scaling on achieved cancellation with perfect 180° phase difference.*

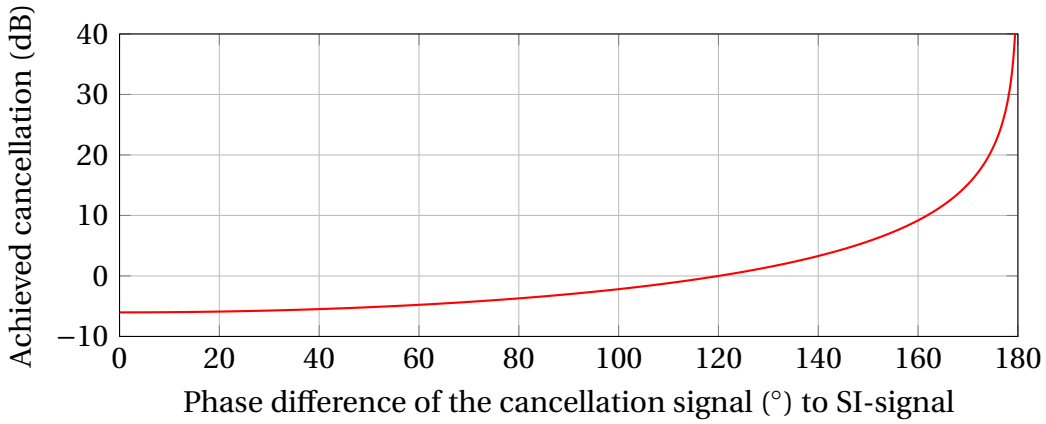

(b) *Effect of cancellation signal phase difference on achieved cancellation with perfect amplitude match.*

Figure 2.9. *Studying cancellation signal phase and amplitude accuracy requirements for cancellation.*

The aim of the full-duplex transceiver is to cancel the SI all the way down to the noise floor. In practice this can require more than 100 dB of cancellation of the TX-power.

2.7.1 Digital Cancellation

Digital cancellation is presented here in very high level as the focus is on the analog cancellation. The principle of the digital cancellation is the very same; create a replica of the SI signal and subtract these samples from received signal.

The assumption that the SI signal is perfectly known because it is own transmission turns out to be too simple an approach [3]. As described previously the signal will go through many components in TX and RX chains before finally being back in digital domain. All the components affect the phase and/or amplitude or even distort the signal and all these changes must be taken into account in digital filtering [19]. The phase and amplitude changes can be tackled quite straightforwardly for example using pilot signals and measuring the change in amplitude and phase [3]. However, the distortion is far more delicate as it introduces frequency components to the SI signal that are not present in the clean BB TX signal. Hence, in order to cancel these components as well, they must be generated artificially. The strength of the intermodulation products depends strongly on the used PA and TX power. Low-cost PAs can have as bad as 15 dB separation between the *3rd order intermodulation distortion* (3rd IMD) and the main signal power levels.

Finally, it cannot be assumed that the SI would be static. As already mentioned, the changes at the proximity of the antenna will change the reflected power and the SI respectively. All these changes must be tackled and the solution is adaptive filters. Those are filters with feedback structure. They minimize the given error function. Adaptive filters are commonly used for example in acoustic echo or noise cancellation. Here the application is the same as the SI can be considered as own echo. There are several adaptive filtering algorithms and two examples are *least mean squares* (LMS) and *recursive least squares* (RLS).

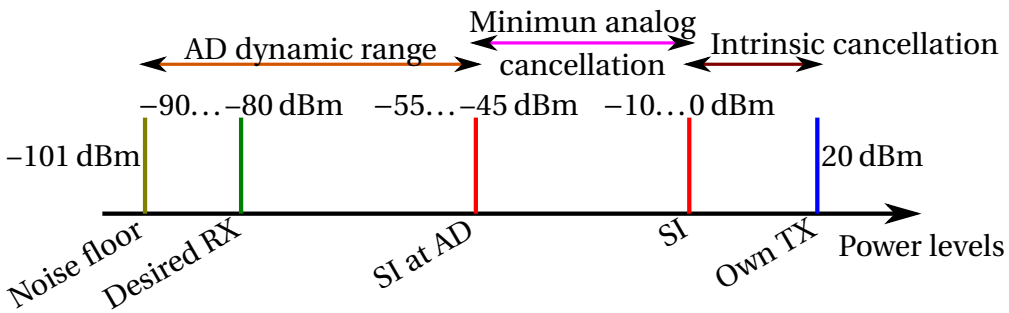

Figure 2.10. *Overall power levels in full-duplex cancellation. Example values are computed for WLAN example.*

2.7.2 Analog Cancellation

Part of the TX signal can be coupled to RF-canceller using couplers. Coupler is a passive device that takes a "sample" from the input signal and passes it through. The insertion loss for the passing through signal depends on the coupling factor but with a 10 dB coupler the theoretical insertion loss is already less than 0.5 dB. This insertion loss directly reduces the TX power but on the other hand too high coupling value makes the cancellation power too small. It must be strong enough such that after the analog processing the cancellation power still is greater or equal than the SI power after intrinsic attenuation.

In order to cancel, the delay, phase and amplitude needs to be matched. The delay is highly dependent on the system and cable lengths so it must be adjusted device wise. A transmission line can be used to have a specified delay or a specific delay line component can be used as well. Phase and amplitude can be adjusted by using a phase shifter, attenuator, amplifier or a vector modulator. Amplifiers should be avoided as they increase the noise and can cause distortion to the signal. Phase shifter and attenuator are both separate components whose control can be digital or analog. A vector modulator is a device which does both of the operations. For a limited space a vector modulator is thus a natural choice.

To do the actual cancellation two RF-signals must be summed. This can be done using the aforementioned directional couplers. Again, the cancellation signal is applied to the coupling port in order to minimize the RX insertion loss. This minimizes the TX and RX insertion losses but at the same time requires a very good intrinsic attenuation from circulator and the antenna. Other possibility is to use Wilkinson power splitter [13, p.328] as a combiner which unfortunately is a lossy unless signals to be combined are in-phase and equal amplitude. For example feeding two 0 dBm signals will yield 0 dBm output instead of 3 dBm using an ideal Wilkinson divider.

Finally, in order to track changes in SI-signal a control is needed. Part of the canceled signal must be used as a feedback signal for control network controlling the vector modulator. The control can be done using analog or digital circuits. Here similarly as with digital cancellation an adaptive control scheme must be used in order to minimize the SI-power before LNA.

2.8 Full-duplex transceiver architecture

Based on the discussion in previous sections the direct conversion transceiver (Figure 2.1 on page 4) operating in full-duplex mode is presented in the following Figure 2.11.

New blocks are the digital and RF cancellation as well as single antenna with a circulator. The focus of this thesis is on circulator based full-duplex operation but dual antennas could be used as well.

The analog RF-cancellation signal is taken from the PA output. The motivation for this is to include all possible TX-chain impairments into the cancellation signal. In essence, this makes possible to cancel for example PA-distortion and noise. Study in the reference [19] agrees with this and shows it to be the optimum coupling point.

The details of the cancellation blocks are not shown for the sake of clarity. Regarding to digital cancellation—which is out of the scope of this thesis—an interested reader should consult, for example reference [12]. The RF cancellation will be the focus through the following chapters.

2.9 Current research activity

Several research groups in academia and industry are currently working on in-band full-duplex operation. Here, some of their approaches are briefly explained. The obtained results are compared with the results of this project in the Chapter 4.

Perhaps one of the most well-known research group is based in Stanford University, led by professor Sachin Katti [4]. Recently they have been working on analog RF SI cancellation using two approaches: creating a suitable null at the RX antenna and creating an analog domain *finite impulse response* (FIR)-filter to model the SI channel. In the former approach, presented in [2], instead of relying only on antenna path loss, more intrinsic attenuation is gained by adjusting dual TX antennas to create destructive null at the RX antenna. This can be achieved such that the phase difference on dual TX antenna paths are at opposite phases at the RX antenna. On top of that, active cancellation is done using QHx220 chip which is an off-the-shelf RF noise cancellation chip [20]. The challenge of this design is the required precision of the antenna positions in order to provide adequate amount of cancellation. As can be seen from their Figure 3 [2, p.4], for best cancellation the antenna positions must be matched in millimeter scale precision. Also the antenna transmit characteristics

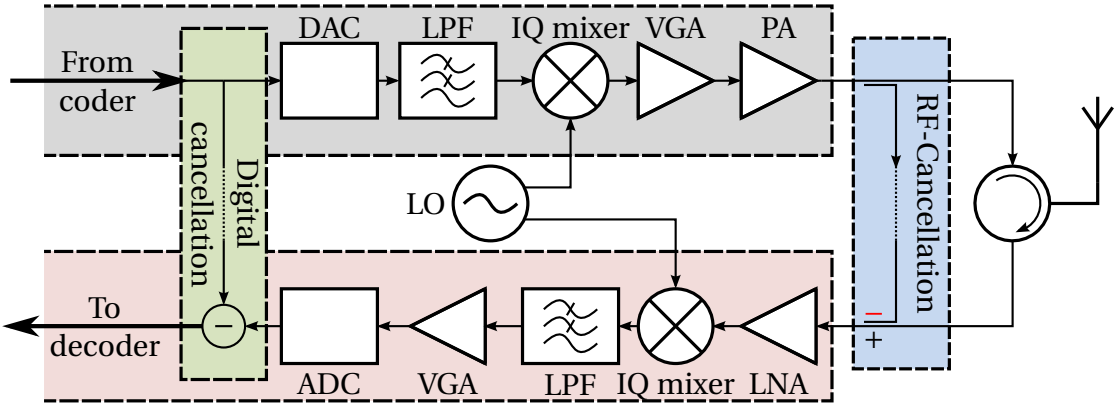

Figure 2.11. *High level block diagram of direct conversion transceiver with additional blocks related to in-band full-duplex operation. The detailed RF-cancellation block is depicted in the following chapter. [8, p.101]*

should be as equal as possible in order to null each other, providing more challenges. Lastly, the QHx220 used as a canceler results high side lobes.

Their more recent approach is presented in [3]. Their setup is based on circulator approach with one shared antenna and active RF-cancellation. The active cancellation uses an eight-*tap* analog filter to modify the cancellation signal to match with the SI-signal. Those taps control only the amplitude. Sufficient amount of those taps with short tap delay difference Δ_{τ_k} allows the phase to be controlled up to certain extent as well. The challenge in this design is the required amount of taps as this requires significant amount of board space for all the required transmission lines (See Figure 6 in [3, p.8]). The control of these taps is externalized and adaptivity is taken into account.

Joseph G. McMichael and Kenneth E. Kolodziej from MIT Lincoln Laboratory present in their paper [21] dual antenna based full-duplex setup using complex taps, i.e. both amplitude and phase control. Their design has a control algorithm which can find globally best settings regarding the output SI power. However, this requires some matrix computation which can be a very demanding operation. Their actual implementation consists of dual tap canceler and here also the control is externalized. The design seems to be still at very early stages and no adaptivity properties are presented.

Binqi Yang et al. from Southeast University Nanjing present in their paper [22] also a vector modulator based full-duplex canceler with dual antenna setup. They have a single tap with accurately matched delay. It can provide good cancellation provided that the frequency response of the cancellation path and SI path correlate well. Multipath reflections can easily alter the SI frequency response which then poses challenges to single tap canceller reducing the amount of obtained cancellation. Their adaptivity is based on monitoring the output power with a log-detector and then controlling the vector modulator.

Lastly, a completely different approach is done by a company called Photonic Systems Incorporated [23, 24]. They propose an optical substitute for the circulator providing in order of 30 dB to 40 dB of isolation over decades of bandwidth, a very impressive result. It is not worth optimizing the circulator isolation unless the antenna return loss can be improved as well. Here, the problem is taken care of by using balanced TX signal and single-ended RX-signal. By connecting a single-ended antenna to the other of the balanced ports and a suitable load (they call it a pseudo-antenna) to the other balanced port, the problem of reflected power from the antenna can be compensated. Note the similarity with electrical balance networks. Currently the design is fitted into a 19” rack enclosure and thus is not compact [25].

2.10 Summary

In-band full-duplex provides significant advantages with respect to classical FDD and TDD techniques. The challenge in the realizations is the strong SI coupling to the receiver. This needs to be canceled both in digital and analog domains. Due to enormous requirements in dynamics, the analog impairments can severely limit the performance. With careful design and joint analog and digital cancellation it is possible cancel the SI completely out as it is presented in recent research papers.

3. CANCELER DESIGN AND IMPLEMENTATION

In this chapter a novel analog RF-canceler is presented, designed and implemented. The word "design" here stands for the process of making an actual device from a high level block diagram contrary to starting from a scratch. Lastly, the implementation is explained briefly.

3.1 Proposed architecture and theory of operation

The proposed architecture for RF-canceler is developed in co-operation with Intel Labs. This design is based on what is presented in a paper titled "Simultaneous transmission and reception: Algorithm, design and system level performance" by Yang-Seok Choi and Shirani Mehr [11].

SI-cancellation is similar to audio echo cancellation for example in telephone systems. These techniques are well-known and proven technology. However, audio echo cancellation is done in digital domain but the RF SI-cancellation must be done in analog domain as explained in previous chapter. The aim of this device is to create an SI estimation signal using multiple replicas of the transmitted signal with different delays, adjust the amplitude and phase of those and finally subtract this estimation signal from the received echo [11, p.5994]. The gain and phase adjustment is needed to form a replica of the SI-signal using linear combination of estimation signals. This is similar to the operation of the FIR-filter. Figure 3.1 depicts the effect of available replica signals (taps) and the delay of one strong SI-component on the available maximum cancellation.

The results of Figure 3.1 are evident as more taps with smaller delay difference result in more accurate replica creation and thus better cancellation as was shown in Figure 2.9 on page 15. It would be thus advantageous to have as many taps as possible but here space constraints usually dictate the available number of taps. The diagram on the right is explained such that when the SI-component is between the taps the cancellation performance is optimal. Naturally the cancellation is very strong when the delays are the same. Notice how the performance degrades when the delay is not between the taps.

Here only one strong component was assumed but in reality in the circulator setup at least two strong components are present, see Figure 2.6 on page 12. Additional SI-components can either increase or decrease the interference power. This case was also simulated such that the tap delay difference was varied from 0.3 ns to 2.5 ns and

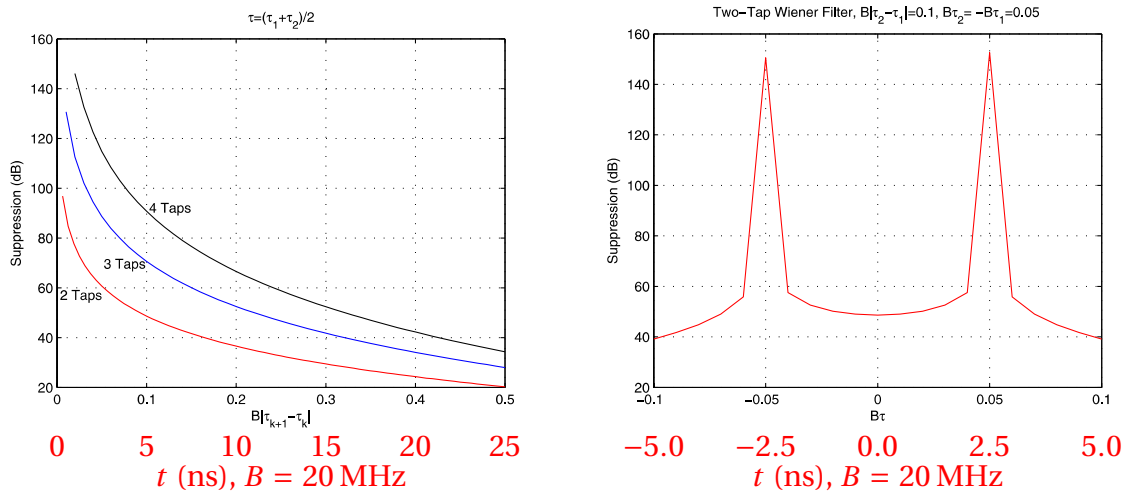

Figure 3.1. *On the left the effect of available taps and normalized tap delay difference on cancellation. One strong SI-component is assumed to be in the middle of the neighboring taps. Normalized tap delay differences for 20 MHz bandwidth B are computed also (added by author). On the right the effect of one strong SI-component position with respect to taps to the cancellation. Here also values for 20 MHz bandwidth are computed. Adapted from [11, p.5995]*

the interference components were such that one was in the middle of the tap delays and the delay of the second component was varied starting from the middle towards the tap. Figure 3.2 shows the results.

Interestingly, the worst case is to have only one component in the middle of the taps. As the second interference component moves towards the tap, the cancellation increases. The results of previous simulations are justified as here also the shorter the tap delay difference the better the cancellation.

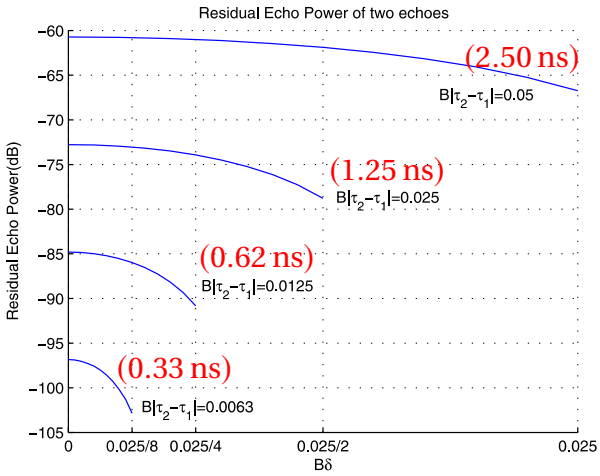

Figure 3.2. *SI-signal consisting of two strong components. Amount of cancellation is simulated against the second interference position with respect the another in the middle of the taps. Different tap delay difference values are simulated and delays in nano seconds are computed for 20 MHz bandwidth by author. Adapted from [11, p.5995]*

Clearly, this approach yields good cancellations provided that the tap delay difference is adjusted well. This is why it is crucial to know the delay characteristics of the circulator and antenna. Based on theoretical analysis presented in previous chapter the only thing still missing is the adaptive control in order to automatically find phase and gain settings for the taps such that the SI-power is minimized.

The self-adaptive operation is achieved using steepest-descent algorithm which is an LMS type algorithm. Mathematically this means that we define a cost-function and then the algorithm aims to minimize this cost function in iterations. In the cancellation scheme a natural cost function is the output power after cancellation. The required mathematical operations are multiplication, summing, subtraction and integration as a form of low pass filtering. All this can be done in analog domain. The update rules for I and Q control for one tap are

$$I: \quad w_{n,I} \leftarrow w_{n,I} + \mu \int \left(x_I(t-\tau_n)z_I(t) + x_Q(t-\tau_n)z_Q(t)\right)\, dt \tag{3.1}$$

$$Q: \quad w_{n,Q} \leftarrow w_{n,Q} + \mu \int \left(x_I(t-\tau_n)z_Q(t) - x_Q(t-\tau_n)z_I(t)\right)\, dt, \tag{3.2}$$

where w is the corresponding IQ *weight*, x is corresponding IQ tap signal and z is IQ feedback signal after cancellation. Individual tap delay is marked as τ_n. The parameter μ is also known as step-size and it controls the convergence speed of the algorithm. Integration is required here to low-pass filter the signal. The circuit cannot cancel the signal of interest because it is not correlated with the transmit signal. Figure 3.3 depicts the block diagram of this analog canceler alongside the control circuit. Detailed analysis of theory of operation can be found from [11, p.5994-5996]

From the Figure 3.3 the taps that are used to create the replica signal by linear combination can be seen. Delay consists of natural propagation delay as well as additional delay. The control block on the right implements equations 3.1 and 3.2. Because this is a closed loop control, i.e. negative feedback based, all the benefits of negative feedback are utilized and makes this control robust against imperfections. Also this circuit is fully analog and thus very fast. The blocks of the Figure 3.3 are analyzed in details on the following implementation section.

One thing worth emphasizing is that this circuit has no constraints of the signal to be canceled, excluding practical things such as power levels. This circuit can cancel whatever is fed to the input of the taps including distortion, noise etc. The only constraint is the bandwidth which needs to matched with respect to tap delay difference. Also this circuit could be used to cancel *Bluetooth* signal from WLAN-receiver or vice versa for example. This is a versatile canceler design.

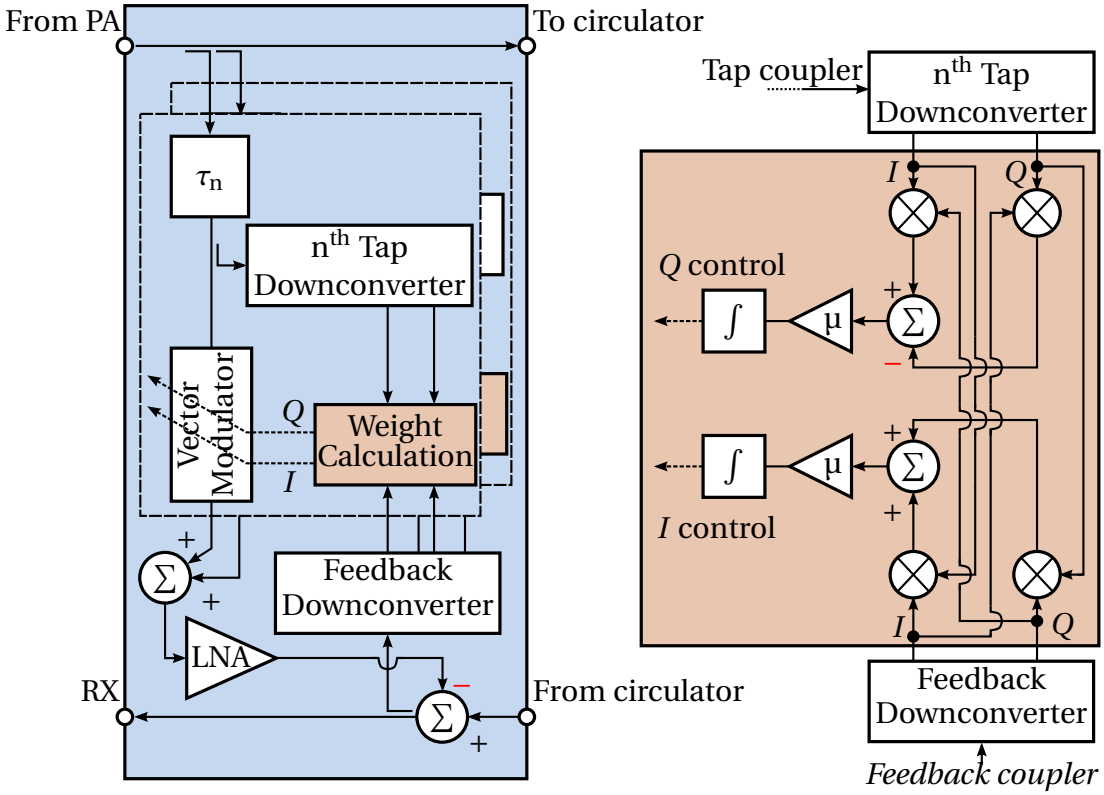

Figure 3.3. *Block diagram showing the analog canceler and the control circuit. This block diagram is a sub diagram of Figure 2.1 on page 4.*

3.2 Implementation

For the actual implementation the amount of taps was fixed to two. As explained in previous section, the tap delays need to be close to the SI delay in order to attain good cancellation performance. It was decided to connect the circulator and antenna using coaxial cables to the board allowing the SI delay to be adjusted by simply using coaxial cables of different lengths. Similarly the additional delay for the second tap is realized using coaxial cables giving flexibility to test different Δ_{τ_k} values. The generality of the demonstrator is not affected as these delay values can be measured and then use fixed value delay lines; components or transmission lines.

3.2.1 Chosen components

The blocks in Figure 3.3 represent the most important components of the canceler. Those are downconverter, vector modulator, LNA and for the control circuit multiplier and integrator. In this subsection those are briefly presented and their choices are justified.

Downconverter is a component that converts the RF signal into BB. RF-signals are difficult to process, they require special transmission lines and they cannot be directly converted to digital domain. Hence, BB processing is used extensively as it is

more convenient and affordable. For example, it would have been almost impossible to make a control circuit that works at RF-frequencies.

Maxim Integrated MAX2023 is used as the downconverter [26]. It incorporates a direct conversion mixer yielding I and Q output at the BB. Here, low noise was one criterion for the chosen downconverter and MAX2023 is specified with relatively low typical NF of 9.6 dB. The output at BB is *balanced* providing robustness against interference. The downconverter requires a 0-dBm LO signal in order to operate. Although it is highly integrated it still requires a considerable amount of external components, mostly for the output filtering network that prevents RF signal leakage into BB. The chip measures 6 mm × 6 mm, has 32 pins and consumes roughly 300 mA at 5 V. Figure 3.4 depicts the downconverter circuit with external components. Two revision of cancelers were built and this photo is taken from second revision canceler.

The adjustment of the RF signal is done using a vector modulator. Hittite Microwave HMC631LP3E was chosen as it is very linear (*input referred 3rd IMD intercept point* (IIP_3) 35 dBm) and it has low output noise floor at maximum gain (–160 dBm/Hz) [27]. The control range for gain is 40 dB and for phase 360° both being continuously controlled using analog I and Q control . Figure 3.5a represents the internal block diagram of the vector modulator and Figure 3.5b the operation principle of IQ-control.[28, p.1]

The vector modulator works such that the input RF signal is split into two components with 90° relative phase shift. The 0° component is multiplied with I-control voltage and 90° with Q-control voltage. Then the components are summed to form single RF output. This processing yields a control described in Figure 3.5b such that the gain and phase can be varied without restrictions inside the dynamic range of the

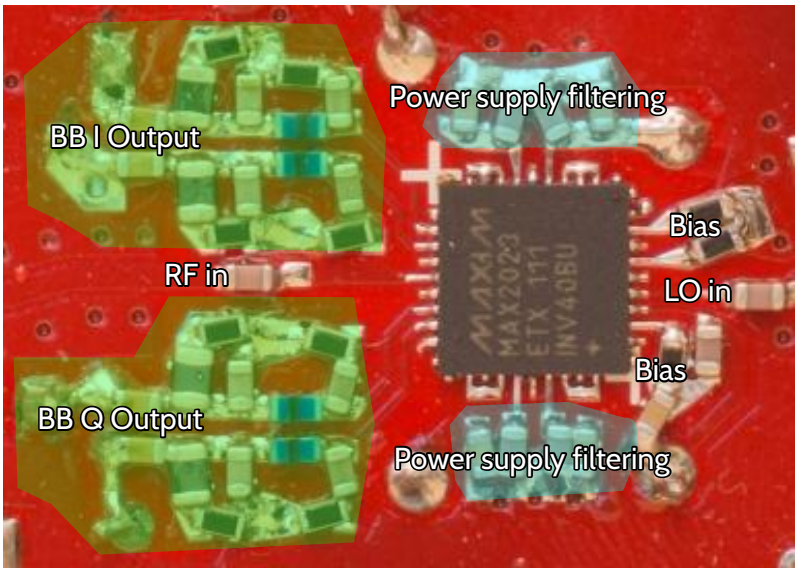

Figure 3.4. *Downconverter circuit with external components. RF and BB traces are* alternating current *(AC)-coupled using* direct current *(DC)-blocks.*

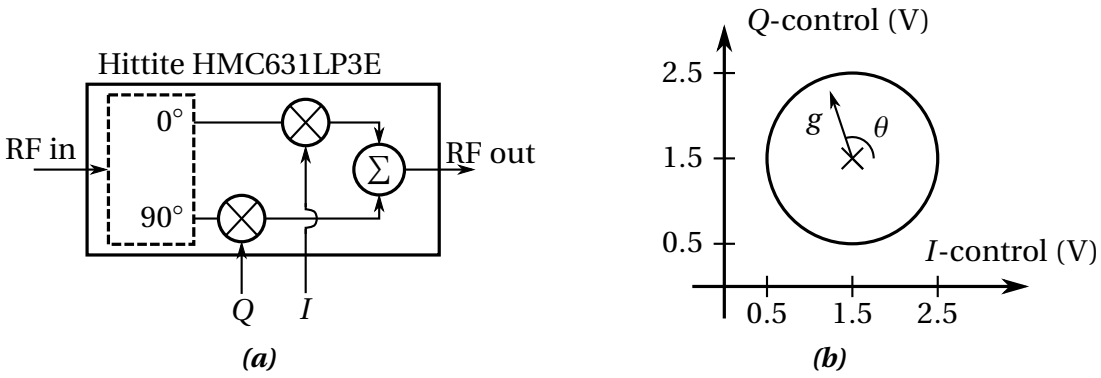

Figure 3.5. *On the left the internal block diagram of the used vector modulator and on the right the principle of IQ-control with nominal voltage levels. The magnitude gain is presented with g and the phase shift with θ. [28, p.1]*

gain control. The minimum gain is at the origin of the circle and maximum gain at the edge of it or outside the circle.[28]

A simple circuit for evaluating the vector modulator was designed and tested prior to the design of the actual canceler. Figure 3.6 depicts the simple canceler. The input power is divided to circulator and vector modulator and a delay line is connected before the vector modulator. The cancellation signal is then subtracted from signal coming from circulator. This board served as an evaluation board and valuable insights of the control and performance were gained prior designing the actual canceler.

The vector modulator requires several external components. The built circuit from revision II board is presented in Figure 3.7. The only drawback of this vector modulator is the maximum gain specified to −10 dB which is a considerable attenuation [27]. There are other vector modulators such as Analog Devices AD8341 but that has only slightly lower minimum attenuation, −8 dB at 2.4 GHz [29, p.7]. However, the maximum input power is significantly lower and thus the Hittite one was chosen. The chip measures 3 mm × 3 mm, has 16 pins and consumes approximately 90 mA at 8 V.

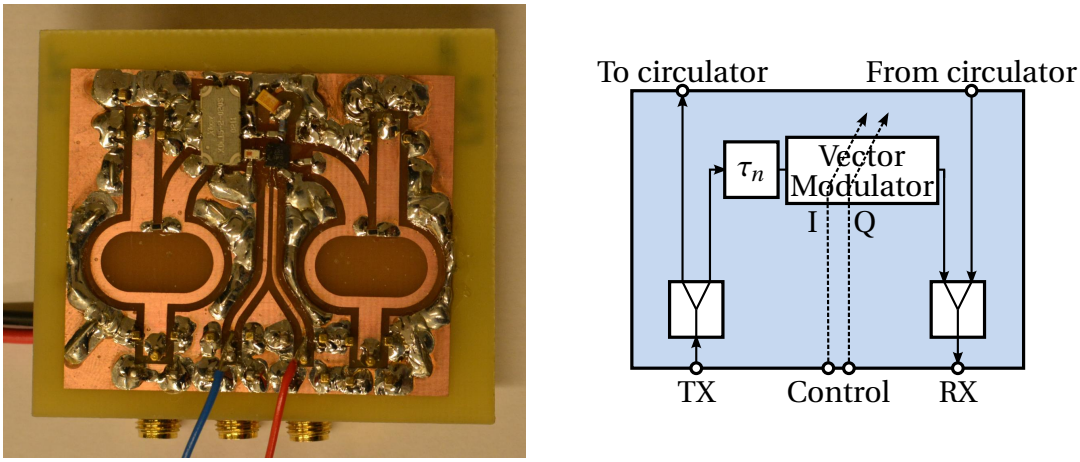

Figure 3.6. *Single tap manual control canceler used mostly as an evaluation board. On the left the realization and on the right the corresponding block diagram.*

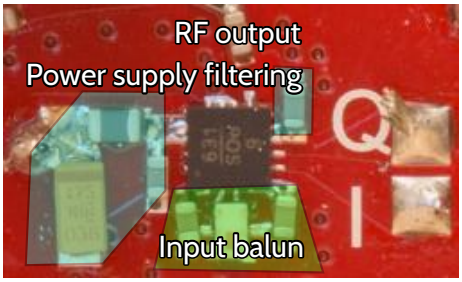

Figure 3.7. *The built vector modulator circuit with external components. Shaded areas in blue belong to power supply filtering. Big pads in IQ-control contains wires to monitor control voltages with an oscilloscope.*

As can be seen from Figure 3.3 there is an LNA at the end of the cancellation chain. It was added to the design at very last phase when it was found out that the minimum attenuation is close to 30 dB for the cancellation signal. Here, two major contributions for the losses come from the 10 dB coupler and the vector modulator (another 10 dB). The rest comes from the Wilkinson dividers and combiners, delay line and other minor components such as balun before the vector modulator. Without an LNA the intrinsic attenuation of the circulator and antenna should be in the order of 30 dB which is a very high demand for the antenna matching. Therefore, to relax the requirements, an LNA is needed at the end of the cancellation chain to boost the available maximum cancellation power. The chosen LNA was Avago Technologies MGA-638P8 which is a high-linearity low-noise amplifier [30]. The IIP_3 point is typically 22.6 dBm which is a very high value. The NF is also very good being less than 0.9 dB. It provides 17.3 dB gain of which then reduces the amount of intrinsic attenuation to less than 15 dB.

The LNA was built also onto a separate small PCB and the measured gain was a bit lower than the specified one. A separate board provides flexibility, again, as it can now be replaced with a short coaxial cable when the intrinsic attenuation is high enough, e.g. when using dual antenna setup.

The most critical components in the control network are the multiplier and the operational amplifier, used in integrator and amplifier circuits. The analog multiplier needs to be fast enough to multiply 20 MHz or wider bandwidth signals. Analog Devices AD835 was chosen as it is highly integrated high performance multiplier [31]. It has bandwidth up to 250 MHz, low noise, balanced inputs and an optional summing node. All these features make AD835 ideal for this project.

Finally the last important component is the operational amplifier. The purpose of the integration network is to ultimately low-pass filter the signal so this component does not have to be any high-speed variant. Instead it turns out that it needs to be a low-input offset voltage type in order to get the high DC-gain integrator to work. This is explained thoroughly in following section along with integration circuits. The chosen component for buffer amplifier (µ in the block diagram of Figure 3.3) and

integrators is Texas Instruments TI OPA2735 having a typical input offset voltage of as low as 1 µV [32].

3.2.2 RF-parts

The input of the canceler, presented in Figure 3.8, was realized as follows. Figure 3.3 on page 24 presents the overall block diagram. Signal is taken to the cancellation network using Anaren 10 dB coupler (DC2337J5010AHF) and then both taps share a common delay line, Anaren XDL15-2-020S. Next, the power is divided using Anaren Wilkinson divider, Anaren PD2328J5050S2HF, and for the second tap there is a coaxial cable interconnection which allows tuning of the Δ_{τ_k}. In revision II canceler the Anaren delay line and Wilkinson divider are omitted and two couplers are used instead. With this small change the insertion loss towards the antenna is decreased by approximately 0.6 dB but the available cancellation power is increased by approximately 5 dB. All of the aforementioned components are *surface mount devices* (SMDs).

Then, as depicted in Figure 3.3, a similar coupler is used to couple part of the signal for the control circuit. The RF-part of the cancellation is simply a transmission line and the vector modulator, Hittite HMC631LP3e. Finally, the two cancellation signals are combined using Wilkinson divider used as a combiner and buffered using Avago MGA-638P8 LNA.

In the output stage, actual cancellation is done using Wilkinson divider as a combiner. After the cancellation part of the signal is coupled back using a directional coupler. The output of the coupler is routed to output RX terminal where for example the spectrum analyzer is then connected. Figure 3.9 depicts the output stage configuration from revision II canceler.

The rest of the RF-part of the canceler consists of LO-signal distribution for the downconverters (Maxim Integrated MAX2023). The LO is supplied externally and first it is split into four. Three outputs are routed to the downconverters and one output is

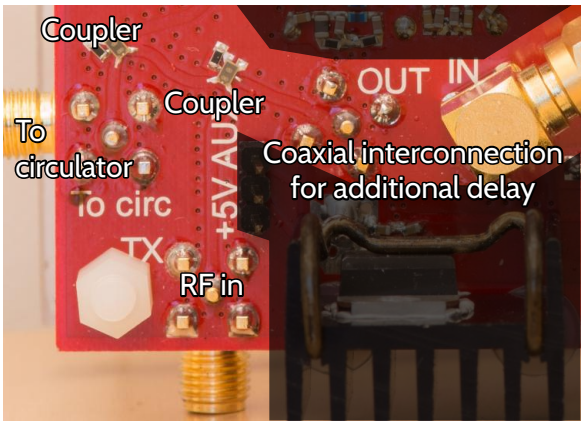

Figure 3.8. *Input stage of the revision II canceler. Shaded areas do not belong to input stage.*

Figure 3.9. *Output stage of the revision II canceler. Shaded areas do not belong to output stage.*

terminated. This routing had to be done such that the LO signals should be as phase matched as possible at the downconverters. The maximum phase difference is only 45° and with greater phase difference the self-adaptive calculation would not work. This is due to fact that the phase of the LO affects the "sign" of the baseband signals and in order to get analog processing work as intended the phase must be the same. At 2.45 GHz one wavelength in the used *printed circuit board* (PCB) is approximately 9 cm. Bearing in mind all this, a phase coherent solution was found such that 2nd tap downconverter lags one wavelength with respect to feedback downconverter and 1st tap downconverter three wavelengths. A short coaxial jumper cable was needed to provide LO signal to all downconverters. When revising the design in ADS the phase difference between the downconverters' LO-input was roughly 10°. Unfortunately due to lack of SMA measurement probes these phases could not be measured.

3.2.3 Self-adaptive control

The self-adaptive operation is achieved using the control network. As explained, it forms an LMS-type adaptive control minimizing an error function which is in this case the feedback signal. The feedback is taken right after the cancellation using a coupler.

First of all, the RF-signals need to be downconverted to BB in order to process the signal in analog domain. Downconverters are used to perform the conversion outputting balanced I and Q signals at the BB. Figure 3.4 presents the implemented downconversion of revision II canceler.

Moving on in the block diagram of Figure 3.3 following are the multiplication operations. Those are performed using Analog Devices AD835 multiplier and the overall multiplication circuit is depicted in Figure 3.10. The transfer function of the multiplier is

$$\text{output} = (X_+ - X_-) \times (Y_+ - Y_-) + Z,$$

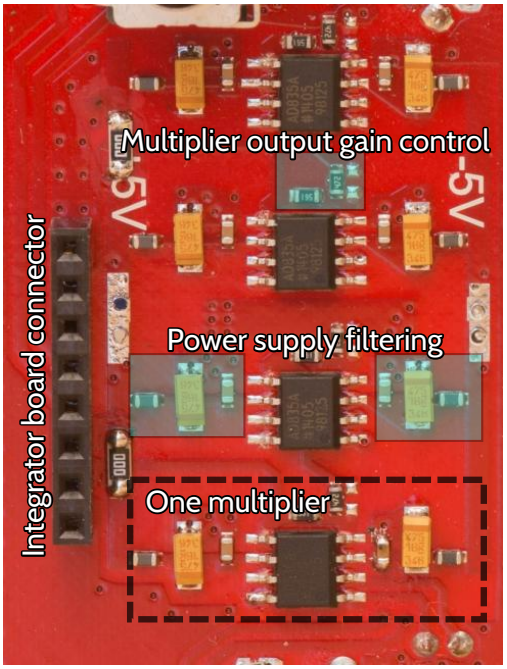

Figure 3.10. *Multiplication circuit for one tap consisting of four multiplication ICs. The summing and subtraction is done using these components as well.*

where X and Y represents the balanced input signals and Z is the optional unbalanced input signal. A total of four chips per tap are used such that the required multiplications are done and the summing and subtraction using these chips. For the subtraction, one input signal in the multiplication was inverted. A balanced signal can be inverted very conveniently by simply interchanging the positive and negative inputs. This yields negative output from the multiplier and finally subtraction after the summing. The summing node could not be inverted as it is single-ended.

The integration circuit was attached to the board providing flexibility and facilitating the component value iteration. This is the final circuit that ultimately controls the vector modulators. The main purpose of the integration is to low-pass filter the control signal.

The buffering can be done either before or after the integration. Integration is done conveniently using well-known operational amplifier circuits. Figure 3.11 depicts the evolution of the integrator circuit in high level.

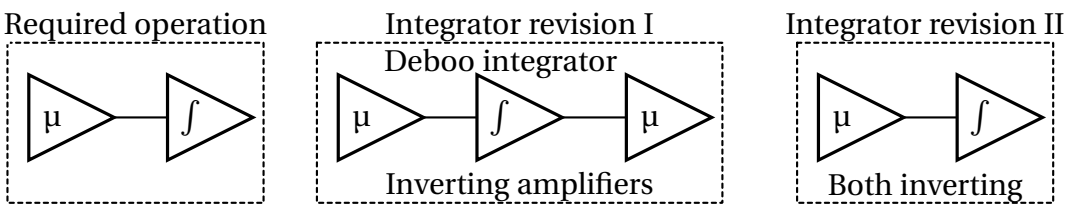

Figure 3.11. *The evolution of integrator circuits in high level.*

As depicted in Figure 3.11, the integration can be done either non-inverting (Deboo integrator) or inverting integrator. First, it was decided to implement a Deboo integrator with dual buffer amplifiers. This allowed studying the effect of having *step-size* μ before and or after the integration. Dual amplifiers are required as they are inverting. The overall system is non-inverting as intended. Figure 3.12 presents simplified schematic for the revision I integrator circuit.

The input consists of the multiplied control signal and an intentional offset-voltage. Offset control is needed because integrators drift quickly into saturation if there is even a small DC-signal present at the input due to high DC-gain. The proposed Deboo and inverting integrators can have 40 dB to 60 dB DC-gain and thus 1 mV can yield 1000 mV unwanted output. Taken into account the useful control voltage range of the vector modulator this is already half of it. Hence, it is of utmost importance to tackle all the unwanted offset voltages by feeding an inverse of it into the input of the integration. Offset is generated by all the active devices in the BB processing, including also the integrating operational amplifiers. Fortunately, there is a special operational amplifier type called chopper amplifier which automatically minimizes their own input offset voltage to µV or nV range. The offset challenge is taken care of by using Texas Instruments chopper operational amplifiers (OPA2735) with a manual offset correction. When the system is powered up, the quiescent output of the integration is adjusted to 1.5 V which is the gain circle null for the vector modulator in use (see Figure 3.5b on page 26). Manual tuning is considered acceptable, hence automatic offset tuning was not implemented.

The actual integration circuit is then quite simple and the integration DC-gain can be adjusted by adjusting the corresponding resistor and integration bandwidth by changing the integration capacitance C_{Deboo}. The gain of the buffer amplifier is conveniently adjusted by changing the feedback resistance $R_{feedback}$.

This circuit was built onto separate small PCB and the system worked with this board. However, the integration DC-offset tuning was difficult and significant drifting

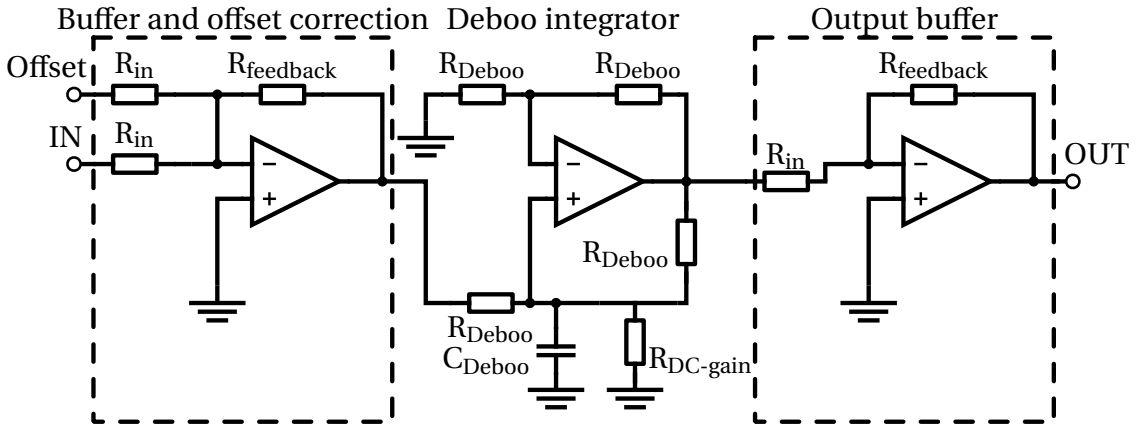

Figure 3.12. *Simplified schematic for the revision I integrator. Filtering capacitors and power supplies are omitted.*

disturbed the control. A second revision integrator (see Figure 3.11 on page 30) was then built using the simpler inverting integrator and an inverting amplifier before the integration. The offset still needs to be corrected before the integration which is why the buffer amplifier is before the integration. Figure 3.13 depicts the second revision integrator with improved offset control.

Figure 3.13 shows that the offset input is now directly to the + pin of the operational amplifier. In fact, in revision I integrators the input stage is a summing amplifier circuit where offset is simply summed with the signal of interest. Here, in revision II integrators, the offset changes the reference level of the input stage which effectively changes the output DC-level of the buffer amplifier. Now there is a significant difference with respect to input resistances for the revision I and II offset inputs. In revision I the input resistance is directly R_{in} due to the inverting amplifier circuit. This is in the order of 1 kΩ to 10 kΩ typically but with the present chopper amplifier these values need to be below 1 kΩ. Because a potentiometer controls the offset, there can be a small drift in the resistance value, for example due to temperature changes. In essence, this change can be the main cause for the unwanted drifting. In revision II integrators, the offset input is electrically behind the operational amplifiers input impedance which is in the order of mega ohms typically. Hence, a few-ohms drift in the potentiometer resistance is insignificant. Figure 3.14 depicts the latest integrator, revision II.

The controls of this board are from top left: fine control of offset, coarse control of offset and DC-gain of the integrator. The red dip switches control the integration bandwidth such that each of the switches adds to the capacitance and thus lowers the bandwidth. These adjustments can be done on-the-fly. All in all four circuits are present for two tap IQ-control. Figure 3.15 demonstrates the control effect on the amplitude response of the integrator.

The revision II performs very well and the drift is minimized considerably. Also the tuning of the offset is more straightforward than with the revision I integrators. There

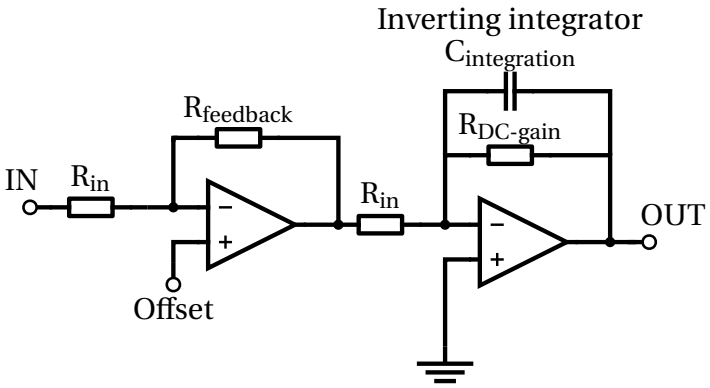

Figure 3.13. *Simplified schematic for the revision II integrators. Filtering capacitors and power supplies are omitted.*

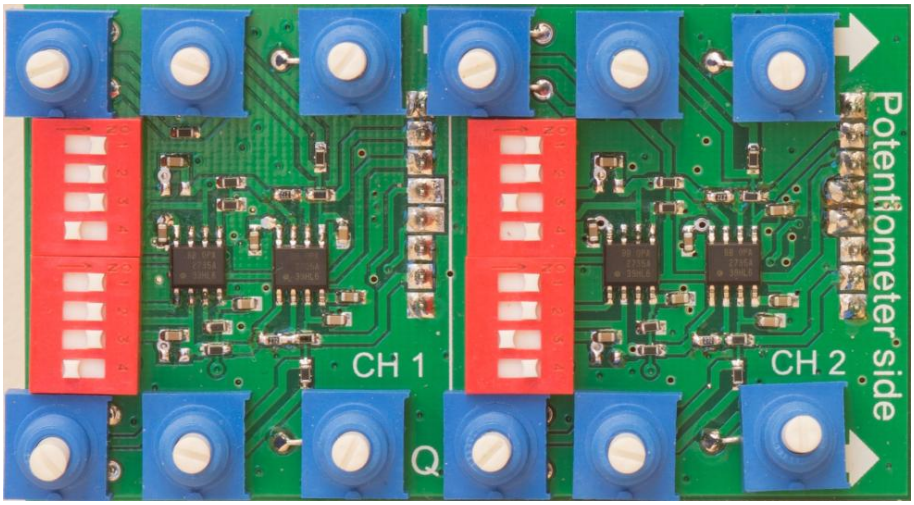

Figure 3.14. *Revision II integrators built. Two integrators are built on the same board in order to connect this board to main board in a robust way.*

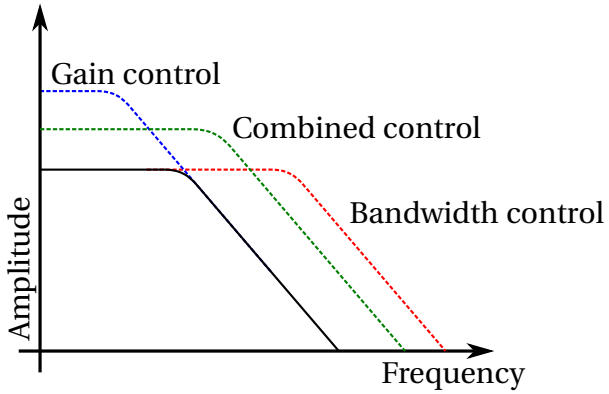

Figure 3.15. *Designed integrator control.*

was a *schmitt-trigger* type effect when tuning the offset and cause for that remained unknown with the revision I integrators.

3.2.4 Built canceler

Two revisions of cancelers were built. Figure 3.16 depicts the first revision canceler. The photo was taken during the building process but the assembly is almost completed.

The system was built on Arlon 25FR which is optimized for RF-boards. It has relative permittivity ε_r of 3.58 and dissipation factor δ of 0.0035; both specified at 10 GHz. The transmission lines were designed using ADS with electromagnetic simulations such that the *characteristic impedance* is 50 Ω at 2.45 GHz. The lines turned out to be quite wide consuming lots of space on the board. This is due to fact that the lines were changed from microstrip to co-planar waveguide with ground type structure without changing the original width of the microstrip line. For the second revision board it was decided to design directly co-planar waveguides with ground as transmission lines. It is optimal for mixed signal boards as it can be made quite narrow and it is well

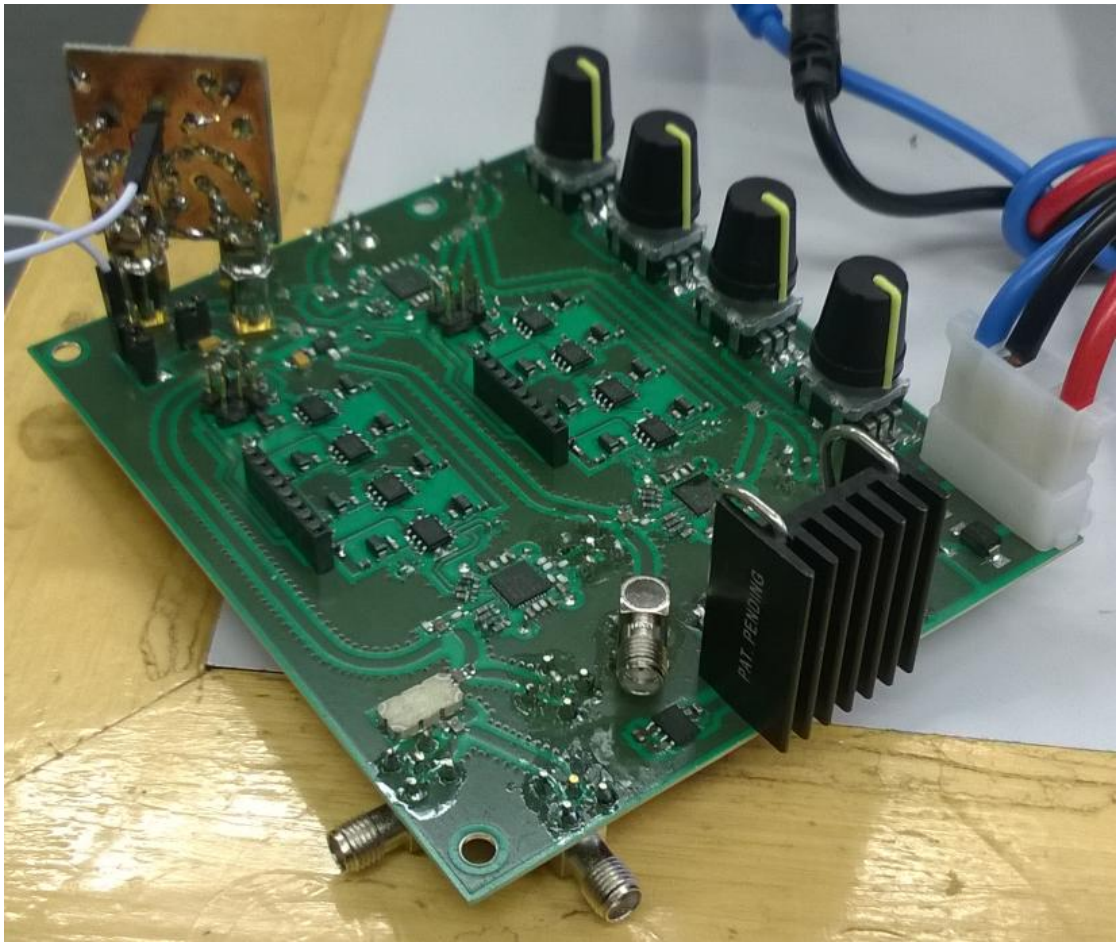

Figure 3.16. *Revision I canceler built. The external LNA board is connected and the open sockets are for the integrator boards.*

protected from causing and receiving interference by a dense *via* fence. Figure 3.17 depicts the transmission line designs for both revisions. The thickness of the PCB was 0.8 mm and 1.5 mm for revisions I and II, respectively. The thickness was increased for robustness.

For corners and curves specific bend or miter values had to be used in order to minimize parasitic effects and maintain 50 Ω characteristic impedance. Consulting [13, p.209] yields bend radius to be $\geq 3w$, where w is the width of the transmission line, or when using acute angles miter value of $1.8w$.

Detailed high-resolution photos of the built revision II canceler are shown in Figure 3.18 on page 36 and in Figure 3.19 on page 37. There are still a few components not yet explained and those are switches to select manual or self-adaptive control and OFF (non-connected) for the vector modulators. Also an internal power supply was built in order to have all the required voltages created on board for convenience. The power supply was designed by Petteri Liikkanen and different voltages are generated by using linear regulators. There is an over-voltage protection implemented by two zener diodes and also an auxiliary 5 V output for external power amplifier which is

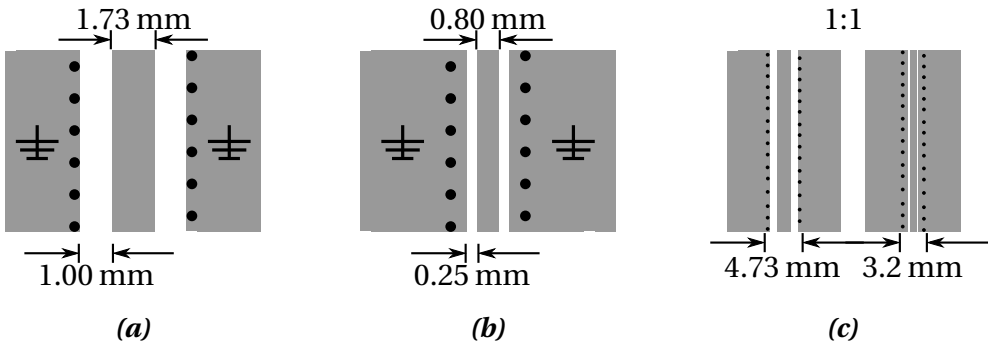

Figure 3.17. *Transmission lines for* ***(a)*** *revision I* ***(b)*** *revision II. Bottom layer consist of a solid ground plane which is not shown in the picture. Black circles represent 0.50 mm diameter vias. On the right,* ***(c)****, revision I and II transmission lines side by side in scale.*

often needed in measurements. The board operates at ±8 V and draws approximately 1300 mA to 1800 mA in total, depending on how many external boards are connected.

3.3 Construction

The boards were built using a re-flow oven of TUT. Re-flow soldering is nowadays commonly used to build commercial boards. The process is as follows. First, the pads of the board are covered with solder paste which is a mixture of soldering flux and very fine solder particles. It is a paste at room temperatures and when heated it forms a solder joint. The flux is chemical which aids the solder to form good joints. The required amount of solder paste is quite small for very small components as in this case. Too little solder paste will not form a good joint and too much solder paste can cause short circuits with neighboring components or pads.

Applying optimum amount of solder paste to very small pads like 0.2 mm × 0.3 mm is very challenging by hand, albeit possible. Commonly, a stencil is used to facilitate this process. A stencil can be made of metal or plastic sheet like transparency. It goes on top of the PCB and its apertures allow solder paste at positions where required. The stencil is attached to the board and then the paste is swept over the holes with a squeegee. This makes the holes filled up with correct amount of paste. Finally the stencil is removed and components can be laid [33, 17.4.6.]. In this design solder paste with particle size of T5, i.e. 15 µm to 25 µm, and a plastic stencil of 125 µm thickness were used.

The components were put then manually using tweezers. By practice, a sufficiently good accuracy can be obtained. The exactly correct position is not required as when the paste is finally molten and is in liquid form, the surface tension will move the part to correct position. The surface tension is strong because the board is covered with solder resist. In fact, the typical green color of the board comes from the solder resist coating. In mass production this process is automated and special pick-and-place robots are used.[33]

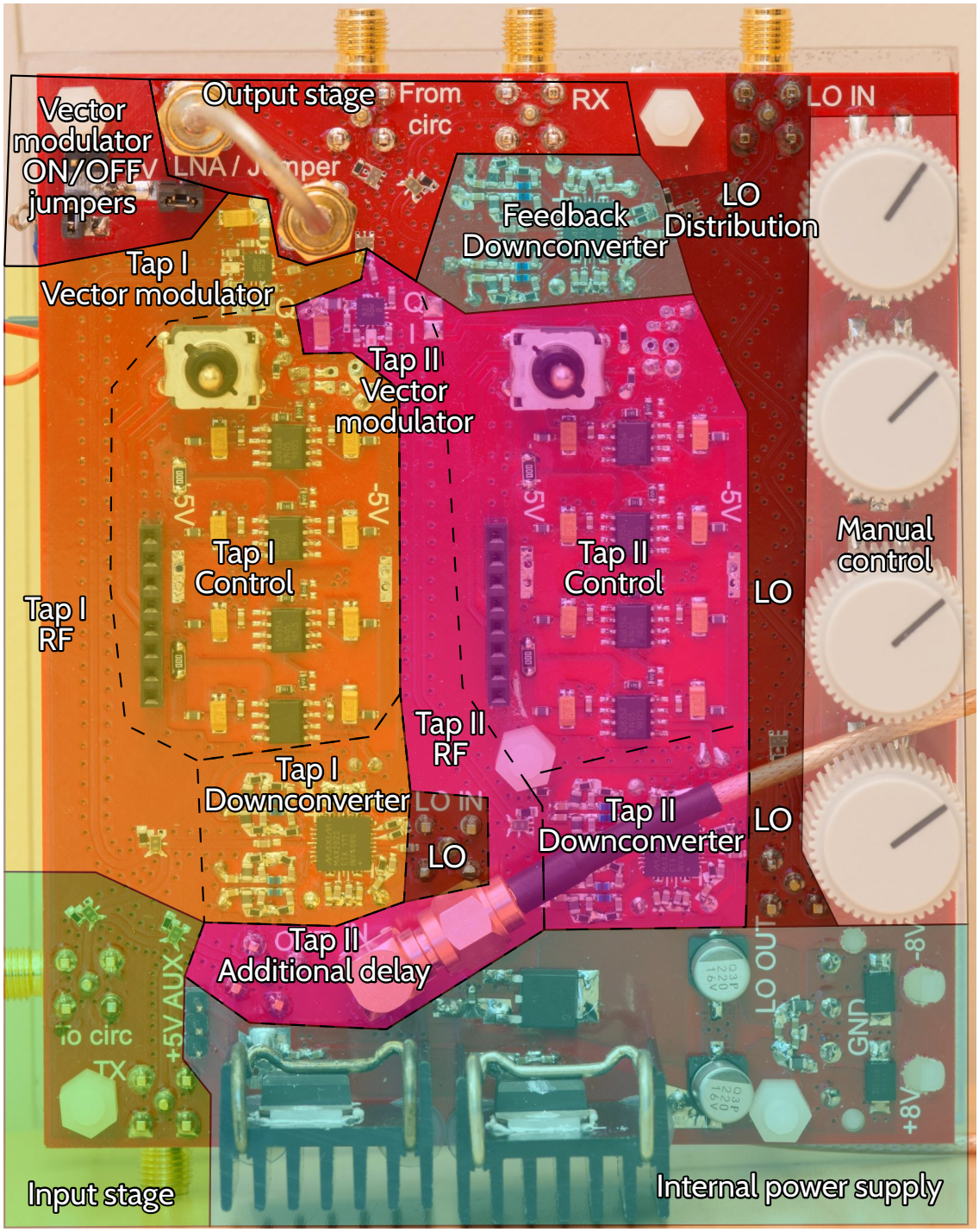

Figure 3.18. *Revision II canceler with blocks from block diagram of Figure 3.3 explained. On the following page is a clear photo without the explanations.*

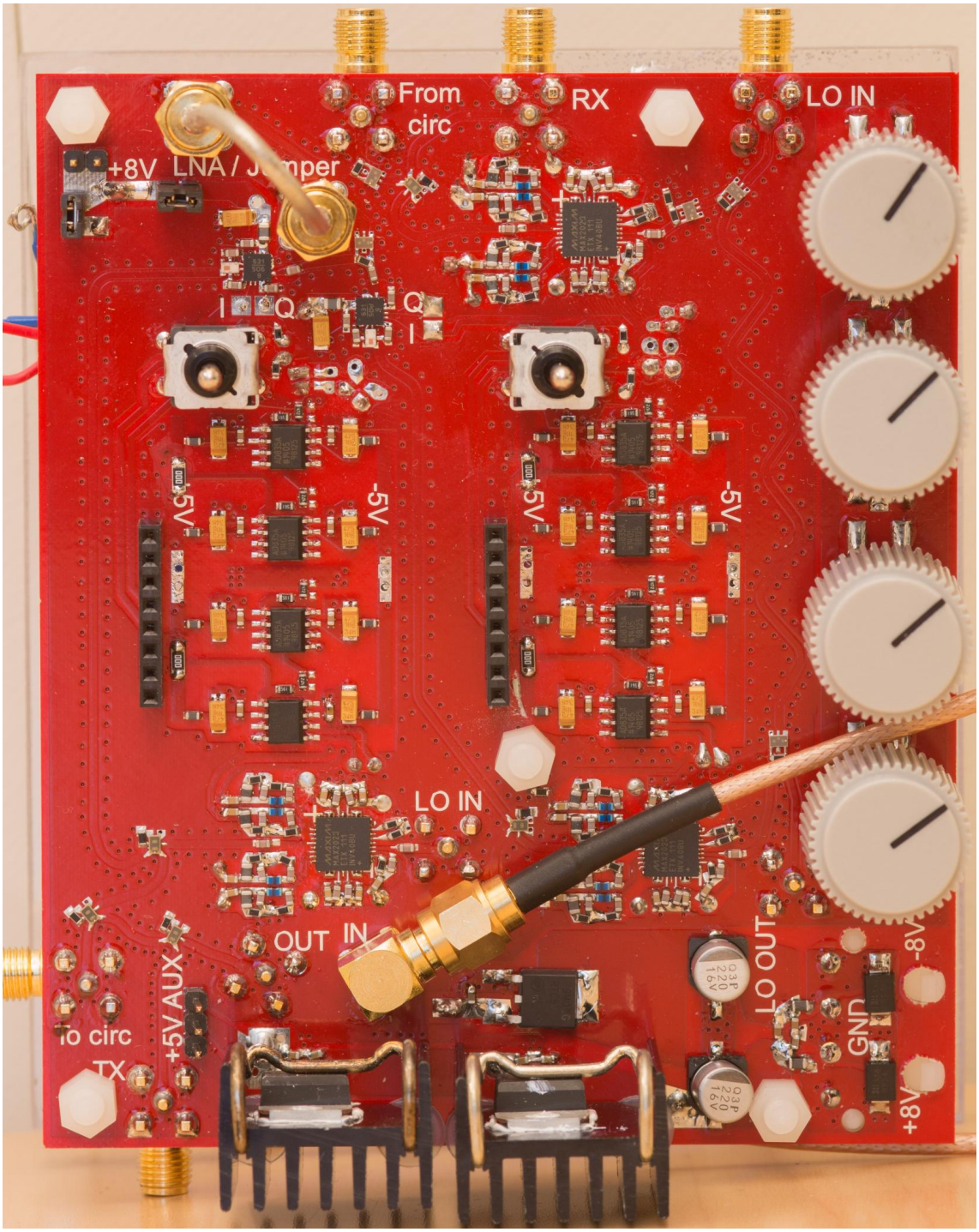

Figure 3.19. *Revision II canceler. See previous page for explanations.*

The overall construction time for the revision I canceler was in total almost two weeks. This was due to poor design of pads which made the building process very challenging. With corrected pads and construction experience from the first revision board the second revision canceler was built in some days. For both of the boards many jumper wires are connected underneath. This was an intended solution, albeit very crude, but it made possible to use only two-layer PCB. For prototyping this is handy as all the traces are directly available. With multilayer boards it is cumbersome to measure signals from inner layers. Also it allowed testing of individual parts of the board before connecting them to the common power supply.

3.4 Summary

A novel analog RF-canceler based on Intel's design was presented in this chapter. Theory of operation and implementation were explained. This canceler is fully analog and capable of adapt itself to variations in SI-signal providing continuous cancellation. The presented design is an early stage demonstration device and it is mainly intended for concept proofing.

4. RESULTS

In this chapter the results obtained from the built cancelers are presented and analyzed. The chapter is organized as follows. First, the operating parameters such as noise level, power consumption, losses etc. are presented. Then the actual cancellation performance in circulator and dual-antenna setups are presented with tracking capabilities. Finally, the results are analyzed and compared with other results.

4.1 Canceler parameters

The power consumption was already mentioned in the previous chapter to be in the order of 1300 mA to 1800 mA depending what additional boards and PAs are connected to it. The operating voltage is 8 V. Therefore, total power consumption was approximately 12 W. This is a high value but the aim of this design has been concept proofing. And, no optimization to minimize power consumption was done. For instance, the regulators—while providing accurate and clean DC-voltage—are not very good in terms of power efficiency. Also the *bias* of the demodulator could have been adjusted to lower the power consumption.

Input and output matchings are parameters of interest. These were measured conveniently using a Rohde & Schwarz ZVL-8 VNA. Figure 4.1 depicts the measurement setups for input and output stage return loss measurements. From the results, shown on *Smith Chart* in Figure 4.2, small spiral loops can be seen which result from reflections. This is most probably due to an impedance mismatch between two closely spaced couplers in the revision II and similarly between the coupler and a mismatched

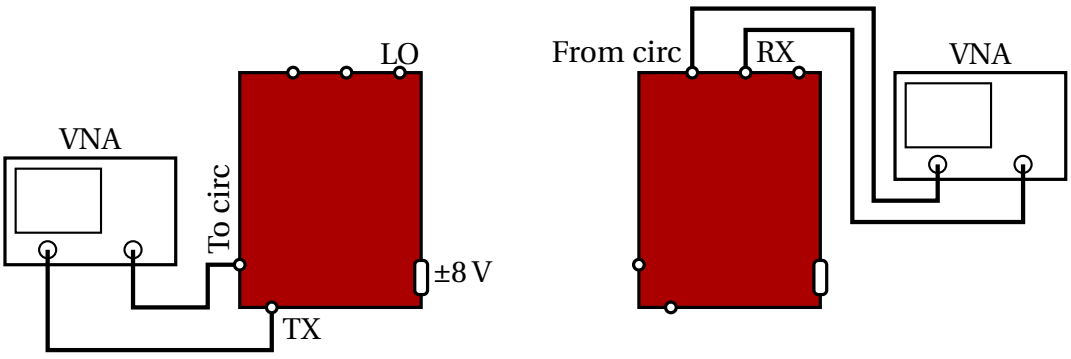

(a) *Input stage.* ***(b)*** *Output stage.*

Figure 4.1. *Canceler return loss measurement setup for* ***(a)*** *input stage and* ***(b)*** *output stage measurements.*

transmission line for the revision I canceler. The revision II has better matching levels than revision I due to improvements in the component pad design. The overall input matching is good for the revision II canceler and no significant insertion loss is due to poor matching.

Similarly the matching for output stages were measured, i.e. ports “From Circ” and “TX”, and results are presented in Figure 4.3. Here, for the revision I canceler the reflection coefficient is very good for the port coming from circulator and good also for the revision II both being clearly better than 10 dB. However, the actual output matching, “RX”, is not very good being less than 10 dB for both of the revision. For the revision II canceler the worse matching is likely due to an error in the co-planar waveguide design. Also, although guidelines given by the manufacturer for the small SMD couplers were followed, the transition from chip to transmission line might not have been the optimum one. To sum up, the matching levels are mediocre and the drawback is for the revision II coupler slightly increased insertion loss in the output stage.

From the same measurements insertion losses for the both TX and RX could be computed. The results are presented in Figure 4.4. Revision II input stage insertion loss is higher by design as instead of one coupler two were used. However, the output stage is the very same and the poor output match of revision II canceler presented in Figure 4.3 can be seen as increase in the output stage insertion loss. Overall, the output stage insertion losses are due to Wilkinson divider used as a combiner ($\approx$ 3.5 dB), feedback coupler ($\approx$ 0.5 dB) and rest coming from the traces and connectors. The standing waves between mismatches are visible similarly as in the previous Smith Charts.

Canceler output noise was measured using revision II canceler all inputs terminated and without the cancellation LNA, see Figure 4.5. The expected noise level was estimated to be below the spectrum analyzers noise floor and hence an LNA was required to be able to determine the cancelers noise floor. The only active device in the RF-path is the vector modulator whose noise will be ultimately at the RX-port. At 2.4 GHz in room temperature the output noise floor is roughly at –164 dBm/Hz [27, p.3]. As there are two vector modulators, their noise powers are summed in the Wilkinson combiner. However, this summing is lossy and therefore after the summing the noise floor is the same. Finally, the signal is connected through the cancellation chain to the RX-port and this insertion loss is very similar as the orange trace in the Figure 4.4. The noise floor at the RX-port is thus expected to be order of –169 dBm / Hz. Figure 4.6 presents the measured and compensated output noise of the revision II canceler.

Compensation here means correction done to the raw measured data. As mentioned earlier, the output noise was measured through an LNA, HD24089, with gain of 22 dB and NF of 1.8 dB. Also, as setting very narrow *resolution bandwidth* (RBW)

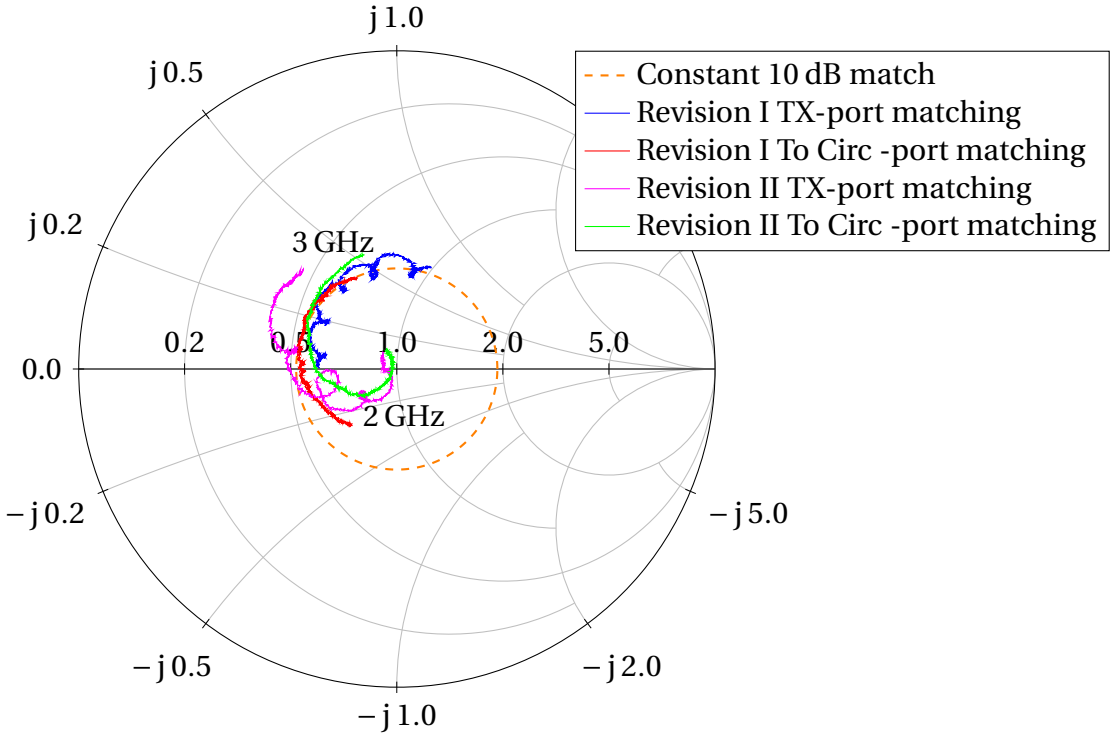

Figure 4.2. *Measured input stage matchings for revisions I and II. Also shown a constant 10 dB matching circle such that points inside the circle are matched better than with a 10 dB return loss.*

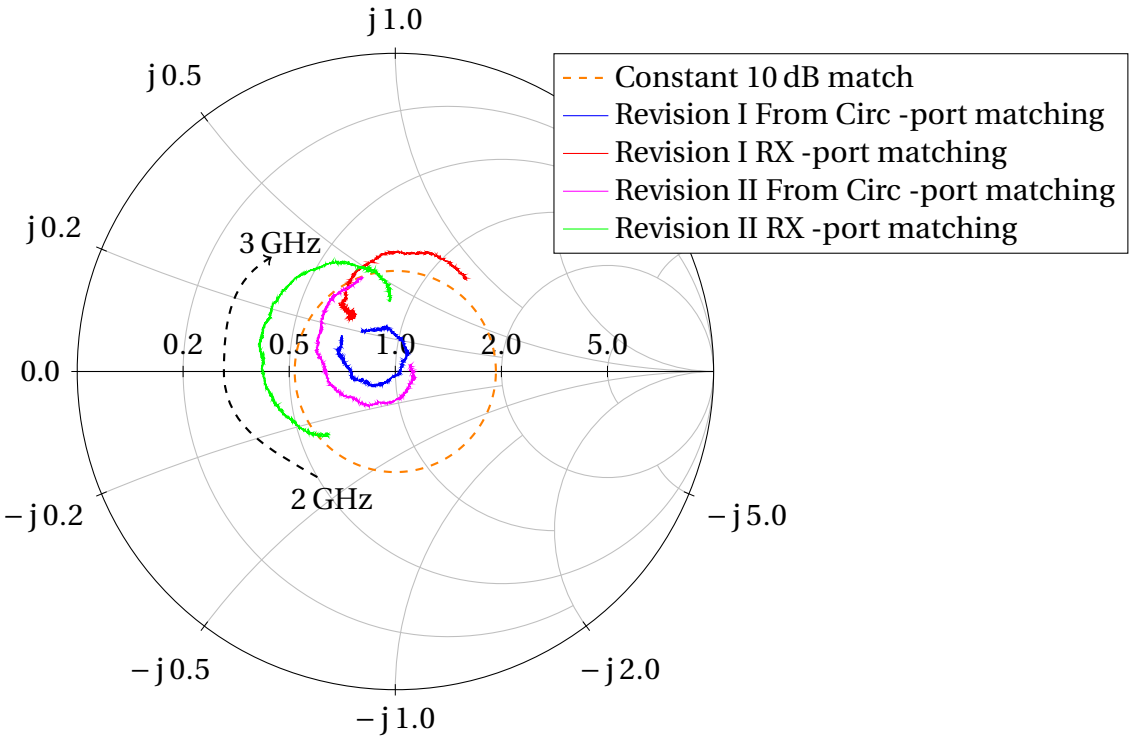

Figure 4.3. *Measured output stage matchings for revisions I and II. Also shown a constant 10 dB matching circle as well as sense of increasing frequency.*

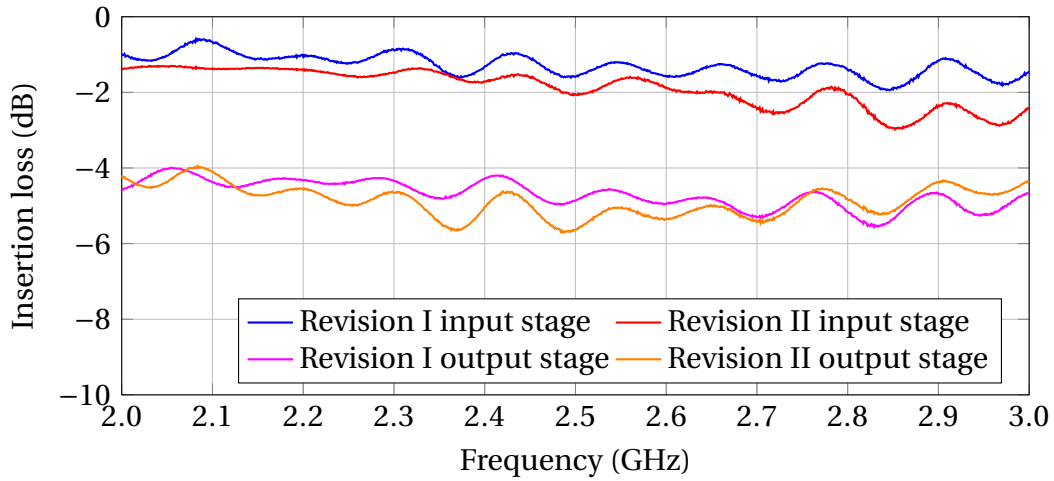

Figure 4.4. *Insertion losses for the input and output stages for both the revisions.*

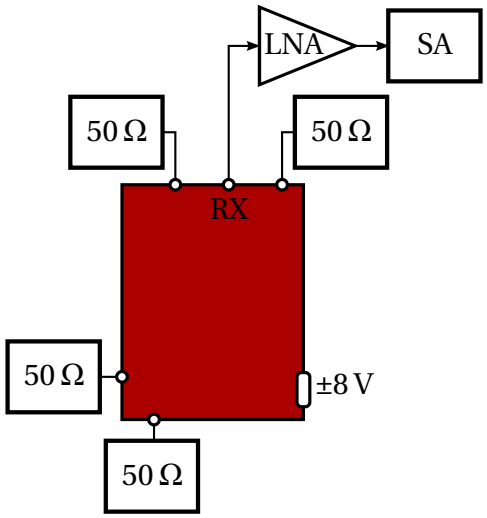

Figure 4.5. *Output noise measurement setup. SA stands for* spectrum analyzer.

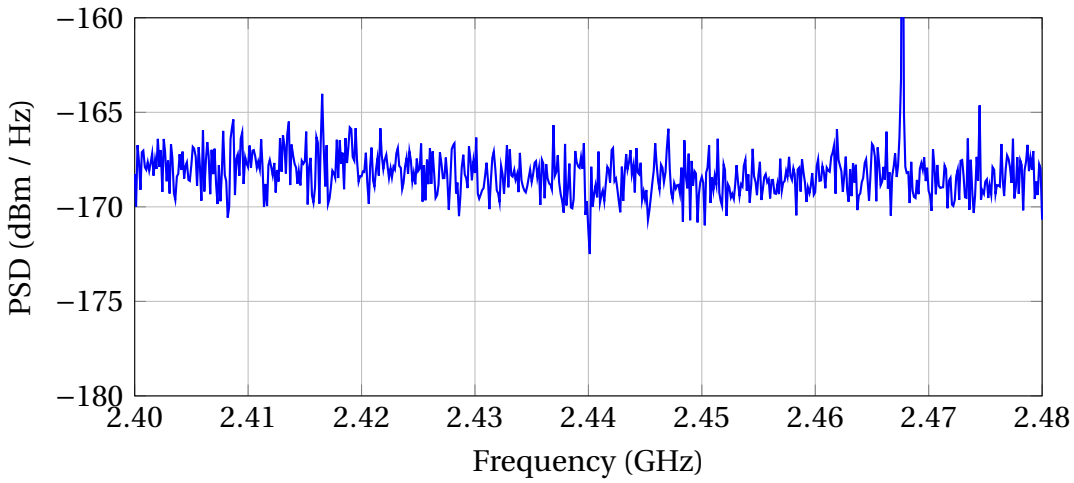

Figure 4.6. *Measured output noise using* root, mean, square *(RMS)-detector. The peak at 2.468 GHz is LO-leakage coming through the canceler.*

prolongs the sweep time of the spectrum analyzer, an RBW of 10 kHz was used. Then, the measured noise floor with one hertz resolution can be computed by deducting the amount of power per each measurement point, in this case by 40 dB. This comes from equation 2.5 on page 11 as now the power spectrum density is wanted as dBm / Hz instead of the measured dBm / 10 kHz, a difference of 10000 which is in logarithmic power scale $10\log_{10}(10000) = 40$. The obtained results correspond well with the value computed based on the data sheet values.

The control voltage conversion is depicted in Figure 4.7. The voltages are presented in time domain in Figure 4.7a such that the RF-signal is turned on at –1 ms. Depending on the gain and bandwidth settings explained in section 3.2.3 on page 29 this convergence time can be adjusted. Setting too fast operation can put the canceler into oscillation whereas very slow control cannot track changes well enough. Here, the convergence time is rather fast being order of 1 ms to 10 ms. The shaded area is plotted also in IQ-plane for both taps such that the plane represents the control voltage range of the Hittite's vector modulator [27]. Note that the calibration was not perfect in this case as the voltages are not exactly at the origin before turning on the RF.

4.2 Cancellation performance

Cancellation performance was measured using two different transceiver setups: *Rohde & Schwarz* (R&S) SMJ-100A vector signal generator with FSG-8 spectrum analyzer and using National Instruments PXIe-5645r vector signal transceiver. The latter one has wider IQ-bandwidth and lower noise floor and thus it suits better the overall system performance evaluation. However, the overall RF-quality, such as phase noise and spurious emissions, is better in the R&S equipment.

Measurement setup diagram is presented in Figure 4.8. Figure 4.9 presents the R&S setup and canceler configured with shared antenna using a circulator. Figure 4.10 depicts the National Instruments *vector signal transceiver* (VST) -based measurement setup with canceler configured to use dual antennas. There is also a *signal of interest* (SoI) generator present which was used in initial SoI measurements.

All the RF-devices were synchronized using master clock derived from the spectrum analyzer in R&S setup and from the external LO-generator in National Instruments setup. The VST is capable of exporting the LO signal and in that case no synchronization is required as it is done already internally. Synchronization is required to align different devices to work exactly at the same frequencies.

Figure 4.11 on page 46 presents cancellation performance measurements conducted using revision I canceler board with revision II integrator. The canceler was working in a hybrid mode such that the other tap was in self-adaptive mode and the other in manual mode. With this control usually the best possible cancellations are obtained and such presents the reference cancellations to be compared with fully self-

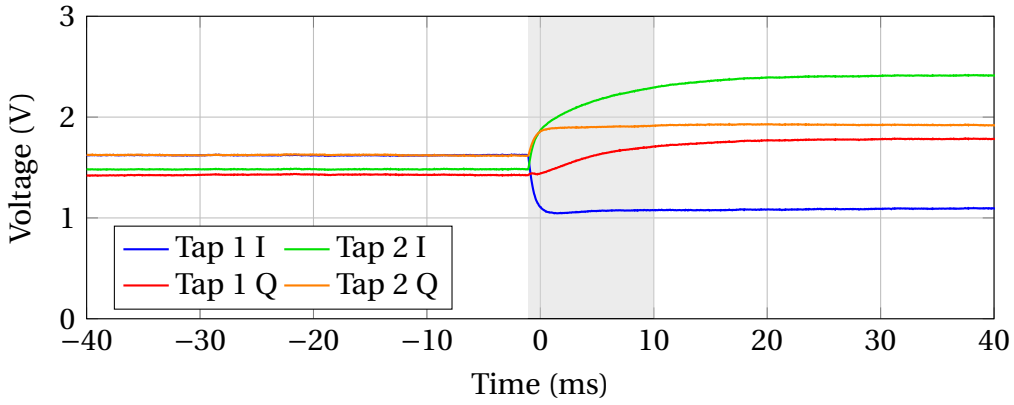

(a) *Control voltage convergence.*

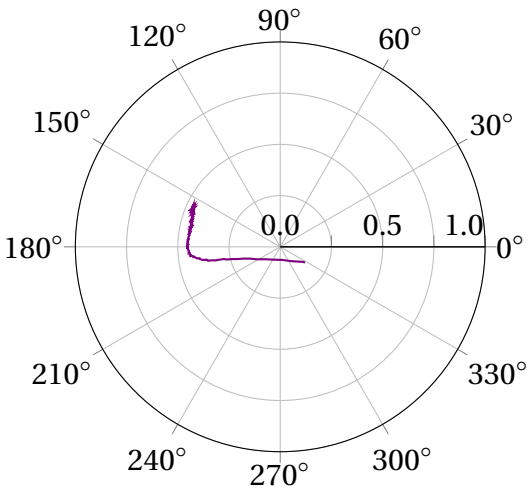

(b) *Tap 1 convergence.*

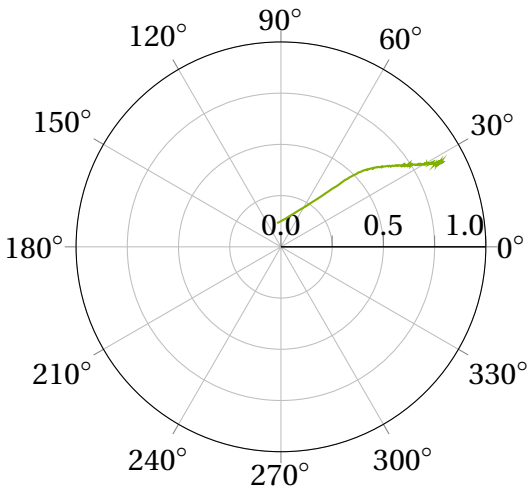

(c) *Tap 2 convergence.*

Figure 4.7. *Control voltage convergence in* ***(a)*** *time domain and in IQ-plane for* ***(b)*** *tap 1 and* ***(c)*** *for tap 2. The IQ plane shows the convergence from –1.1 ms to 10 ms.*

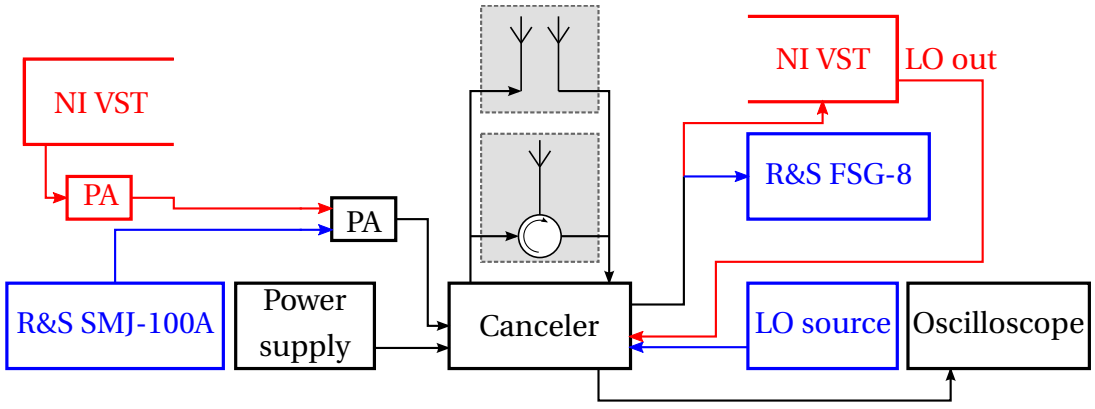

Figure 4.8. *Both measurement setups in diagram level. Specific parts for National Instruments setup are shown in red and for R&S setup in blue. The VST requires a step up amplifier (PA) in order to reach 20 dBm at the canceler.*

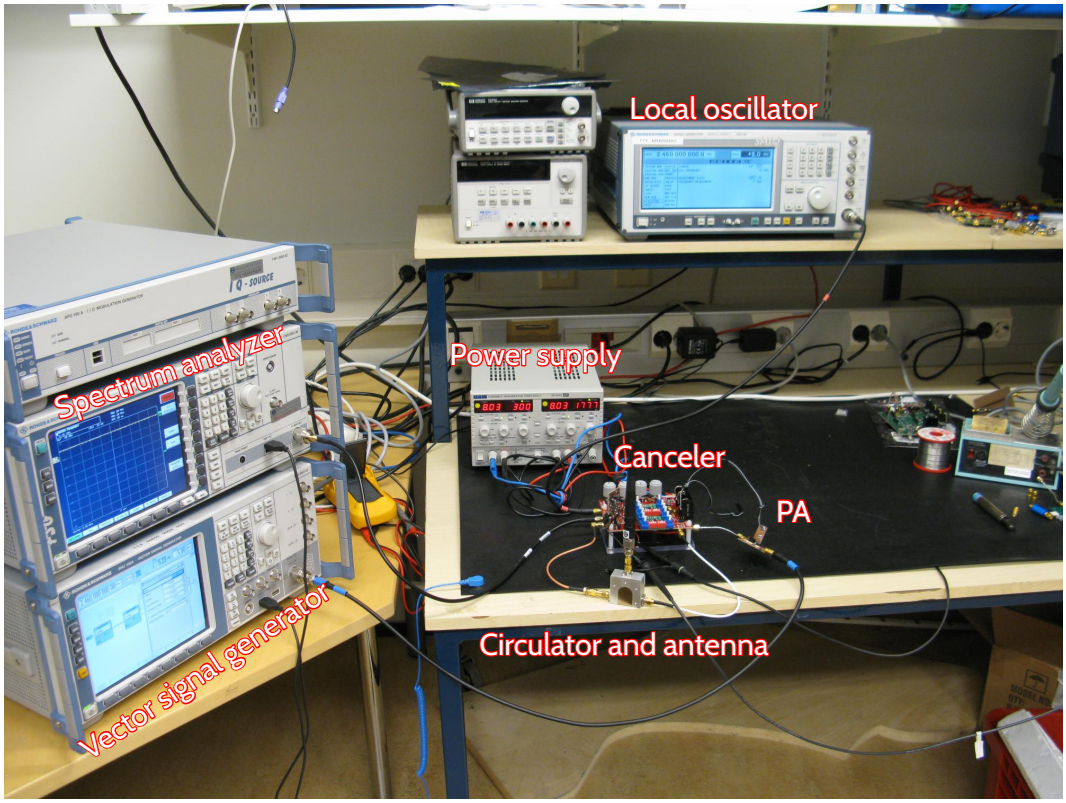

Figure 4.9. *Rohde & Schwarz -based measurement setup.*

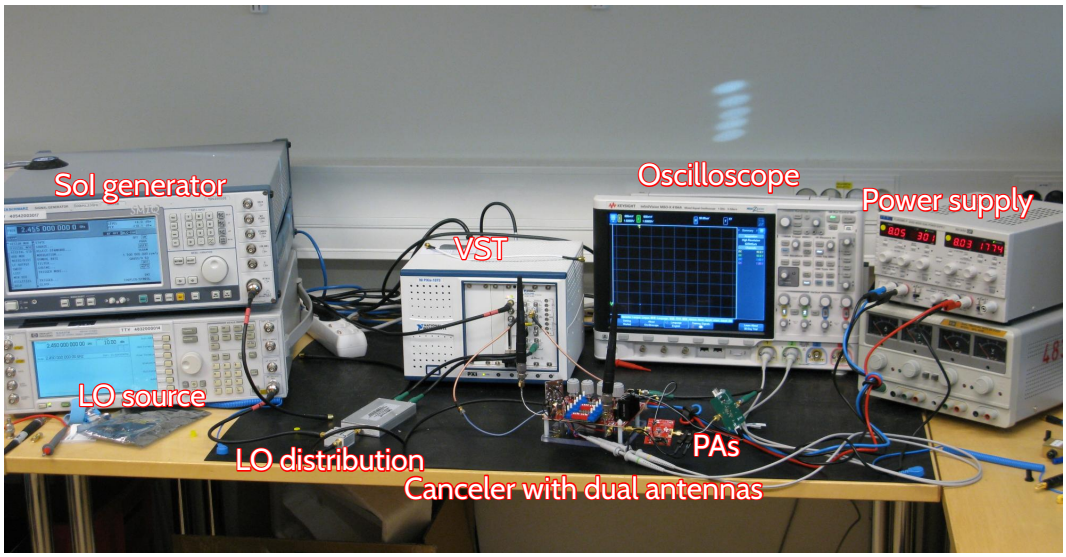

Figure 4.10. *National Instruments VST -based measurement setup.*

adaptive mode. Measurements were conducted using National Instruments -based measurement setup with waveforms of 20 MHz and 100 MHz. An LNA was used in the cancellation chain to increase the available cancellation power.

TX signal here means the signal after the PA at the canceler forward path input. The true TX power is then obtained by subtracting the canceler insertion loss from this power. These two reference points are used for cancellation computations commonly.

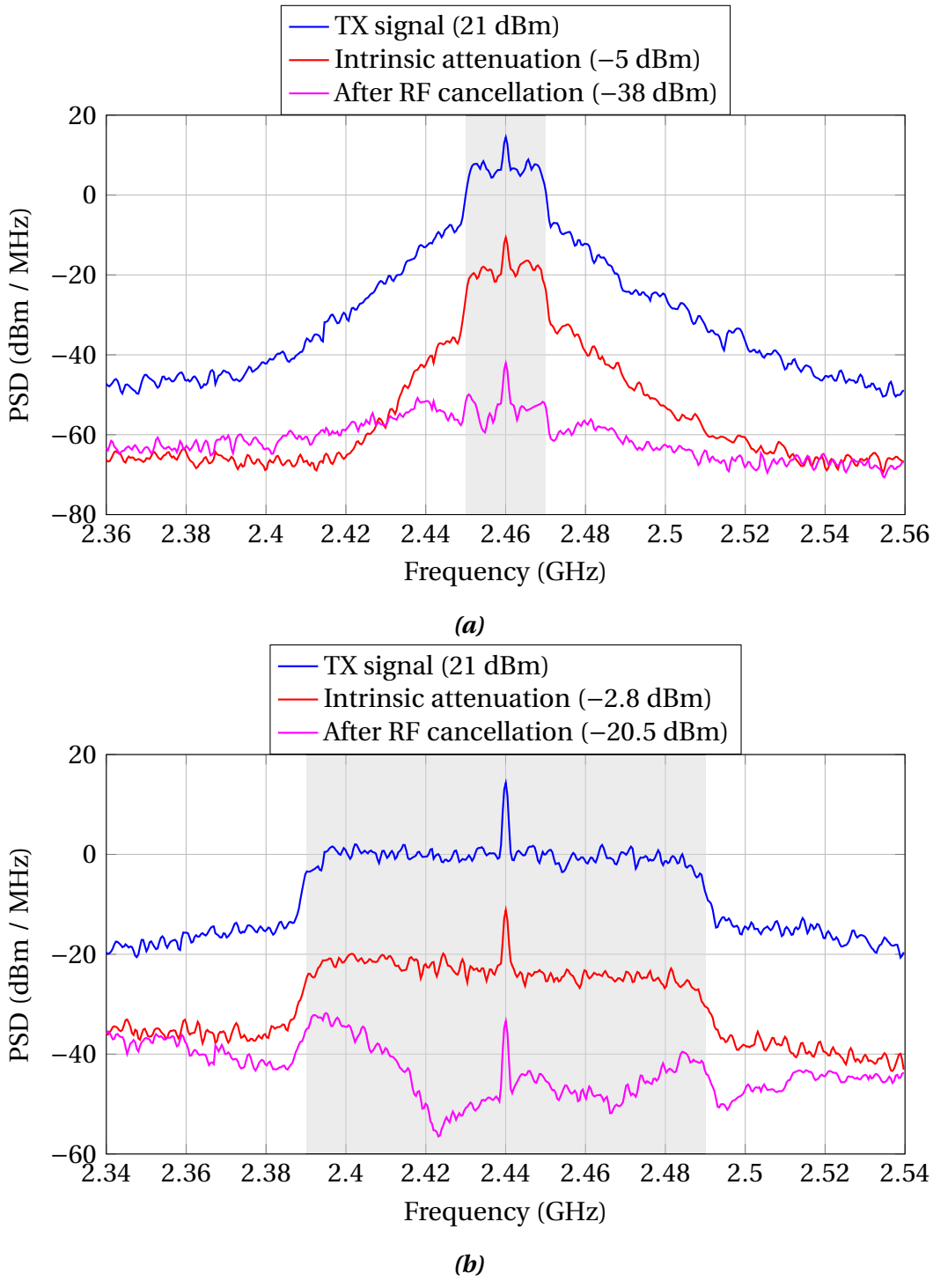

Figure 4.11. *Measured RF cancellation performance with circulator-based shared-antenna device using* ***(a)*** *20 MHz and* ***(b)*** *100 MHz instantaneous bandwidth at 2.4 GHz ISM band. Measurements were conducted using National Instruments VST in spectrum analyzer mode.*

Figure 4.12 on page 48 presents similarly results with dual antenna operation. Here, a special relay antenna developed in Aalto University was used. It consists of two cross polarized patch antennas facing opposite directions thus providing a significant isolation between the TX and RX ports. This isolation can be order of 50 dB or more. Hence, no LNA was used in the canceler and better noise performance was obtained. The canceler was operated in fully manual mode as the power levels after the antenna isolation were already too low to create a control signal for self-adaptive control. This observation led us to design a BB amplifier in order to increase these control signals.

Shown in the Figure 4.12a are the transmit signal, intrinsic attenuation and RF canceled spectra as well as digitally post processed spectra. Note how the 3rd IMD and higher order distortion products limit the cancellation unless it is taken into account. With the non-linear digital cancellation, i.e. taking into account these distortion products, the noise floor of the used receiver, R&S FSG-8, was reached.

In the dual dipole measurement case, revision II canceler with revision II integrators were used. The control was set to hybrid mode again. With shorter cancellation delay than in the revision I canceler the antennas were put closer to each other. The actual measurement setup is presented in Figure 4.10. Also, an external LO source was used in this measurement.

To demonstrate that the SoI is not affected by the SI-signal and vice versa, a simple measurement experiment was conducted. SoI-generator presented in Figure 4.10 on page 45 was used to create additional signal such that it is buried under the SI without any active cancellation and after the cancellation it can be received. Figure 4.13 presents the spectra of this measurement experiment. Here, only analog RF-cancellation was used.

4.3 Analysis of cancellation performance results

Analog RF cancellation can be divided into intrinsic attenuation due to circulator isolation or antenna separation, i.e. passive attenuation, and active attenuation provided by the canceler. The amount of active cancellation is a natural choice to consider as figure of merit for the canceler. However, it is common to combine these two and simply provide a combined analog cancellation value hiding the details. Similarly others count cancellation decibels starting from PA output and the others starting from the actual TX power. Lastly, the RF-canceler output stage always has a non-zero insertion loss. This value reduces the SI **as well as** the desired RX-signal. Bearing all this in mind, the true active cancellation performance should be computed from the actual TX-power without taking into account the aforementioned insertion loss. However, as already mentioned, there will be always some insertion loss so a good compromise is to provide total cancellation including, separately mentioned, this insertion loss. It can be thought as a negative figure of merit.

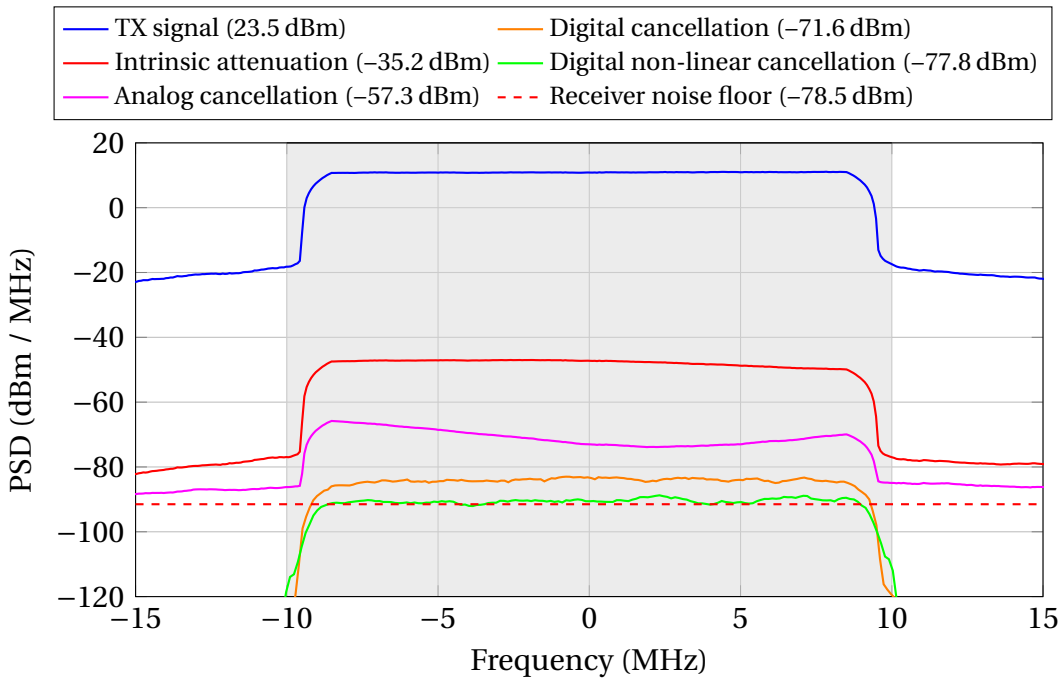

(a) *Relay antenna measurements*

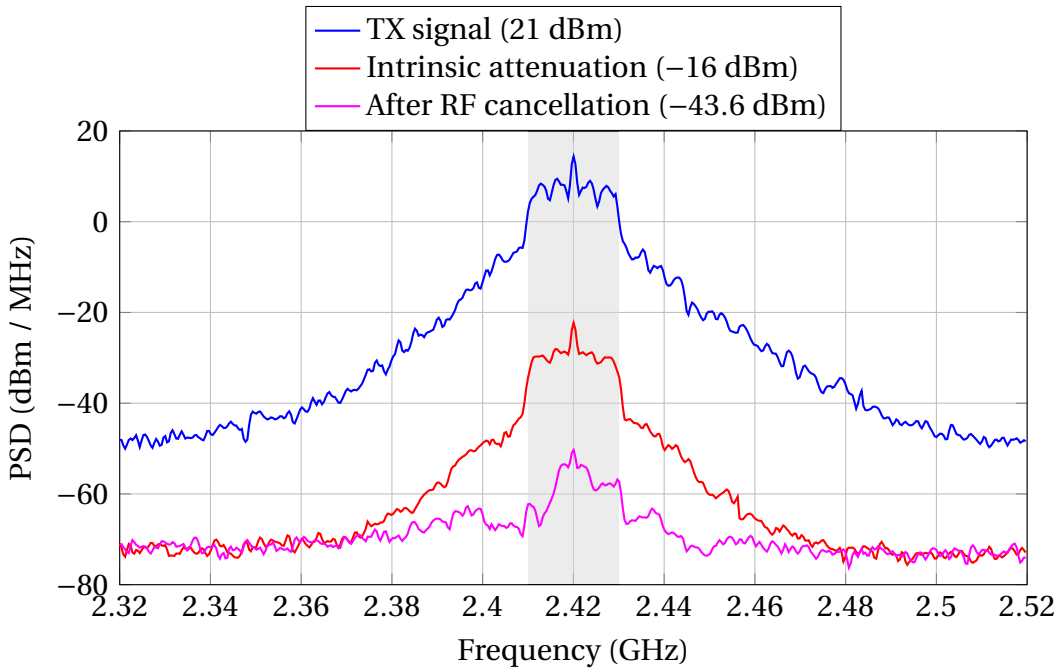

(b) *Dual dipole antenna measurements*

Figure 4.12. *Measured RF cancellation performance with relay and dual antenna based setups. Measurements were conducted using the R&S and National Instruments setups, respectively. For relay antenna measurements, spectra are drawn at BB frequencies including also digital processing results whereas for dual dipole antenna the measurements are conducted using spectrum analyzer mode of the VST.*

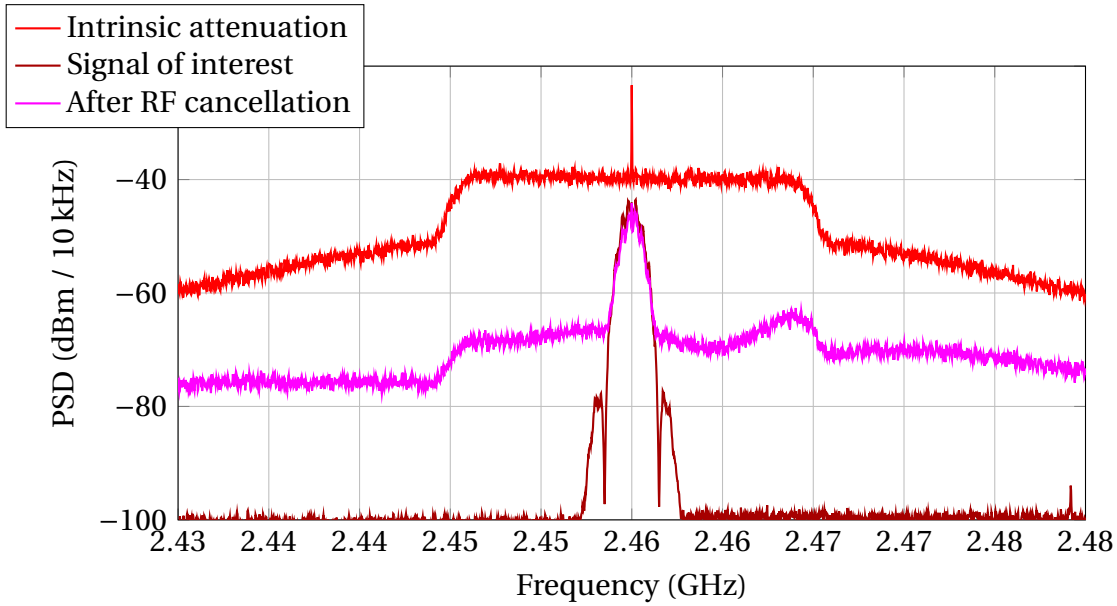

Figure 4.13. *Measured spectra including also signal of interest (SoI), originally buried under self-interference. Note here the different RBW setting (to enhance visibility) with respect to previous measurements.*

In the Figure 4.11a intrinsic attenuation provides roughly 24 dB of isolation (note that the canceler input insertion loss is taken into account). Then the active cancellation can reduce the amount 33 dB more. Both these values include the canceler output stage insertion loss, so the active cancellation is computed correctly. Note also from the TX-signal spectrum how the distortion is visible as a spectral regrowth. Also it can be seen that the intrinsic attenuation is frequently dependent as the SI is attenuated more at the lower than higher frequencies. Finally, the out of the band power after RF-cancellation being higher than the intrinsic attenuation does not necessarily mean that the canceler distorts the signal. Instead, a more plausible explanation is simply that it is residual cancellation signal coming from the cancellation branches.

The high distortion due to the used PA (Texas Instruments CC2595) poses no challenge to the canceler, as can be seen from the spectra. This is one the advantage of the analog cancellation as it has no constraints on the input signal except being at the operation frequency. For digital cancellation this distortion is troublesome as the reference signal is free of impairments. Therefore, other means need to be used in order to cancel distorted signal. Also the analog cancellation can cancel the TX-noise from receiver as it can be considered to be input signal as well.

In the Figure 4.11b intrinsic attenuation provides roughly 22 dB of attenuation with 100 MHz signal. Here, the antenna matching bandwidth is the limiting factor as the circulator can provide good isolation levels over a 100 MHz bandwidth (see Figures 2.4 and A1.1 on pages 10 and 60, respectively). The additional active cancellation is in this case roughly 18 dB which is still a good value considering the wide bandwidth of the signal. It can be seen that here a better cancellation would have been obtained for

narrower bandwidths. This observation agrees with the theory, as wider bandwidth signals require more taps in order to provide equal cancellation, see Figure 3.1 on page 22.

Moving on to dual antenna measurements, results are presented for relay antenna based measurements and for dual dipole based measurements in Figure 4.12. In the relay antenna case the intrinsic attenuation is significantly higher, being 57 dB. Again, input insertion loss is taken into account in this value. Active cancellation is 22 dB. In fact, the canceler would have been able to cancel still more but these settings were used intentionally in order to demonstrate digital cancellation as well. Note how the linear digital cancellation can only cancel down to the intermodulation level. More sophisticated processing is required in order to reach the noise floor.

The dual dipole setup provides also more intrinsic attenuation than circulator based setup. The intrinsic attenuation is order of 35 dB and the canceler operating in hybrid mode is able to cancel actively still 27 dB. All the aforementioned results are gathered to the following Table 4.1 on page 52 for comparison.

4.4 Tracking capabilities

To demonstrate tracking capabilities, a video was recorded showing at the same time the canceler, received spectra and IQ-control voltages. The canceler was set up in fully self-adaptive mode and both of the taps were calibrated to float at 1.5 V when no RF-signal was present. Then RF was turned on and the antenna was interfered with a hand and other objects. Interfering the near field of the antenna changes its input impedance and thus also the reflected power. This is why the canceler needs to be adaptive, in order to track these changes. A few frames from the video are presented in Figure 4.14 on page 51. Different situations are captured and the movement of the IQ-control voltages can be seen from oscilloscope screens.

The measurement videos are available on the Internet at

- `http://www.tut.fi/full-duplex/videos/`

Videos show the cancellation performance and the tracking capabilities when the canceler is run in fully self-adaptive control. The average active cancellation performance of the revision II canceler varies between 24 dB to 34 dB depending on how the antenna is interfered. This is shown in the revision II video on the web page. Nearby objects can also increase the cancellation as in the video the average cancellation is order of 27 dB to 30 dB when no hand is at the close proximity of the antenna.

4.5 Comparison

Results presented in previous sections are gathered into the following Table 4.1 for convenient comparison. It can be said that almost always, unless the antenna is

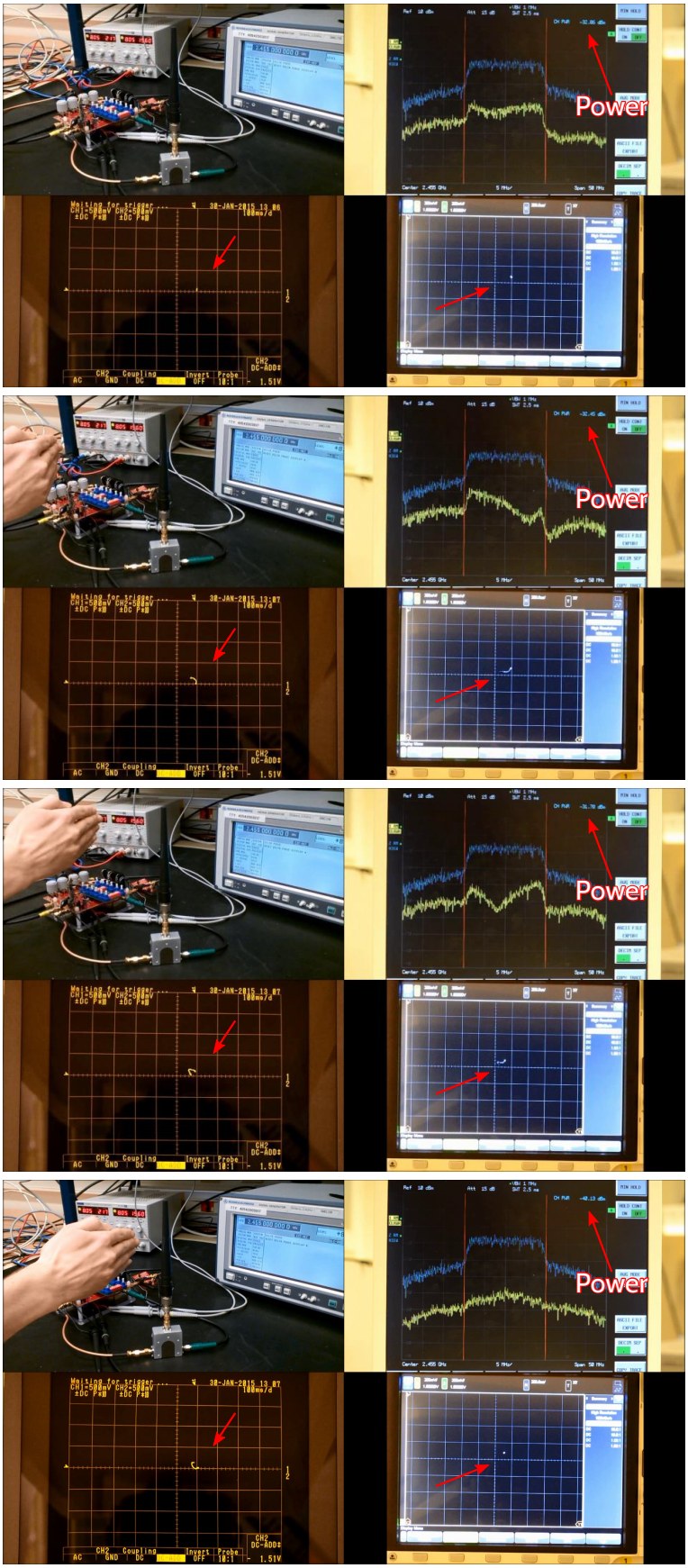

Figure 4.14. *Tracking demonstration, note the movement of the IQ-control voltages. Frames taken from the video.*

exposed under a severe interference, more than 50 dB of total active cancellation can be obtained.

In theory, with two taps and the used tap delay differences Δ_{τ_k} the cancellation should be order of 60 dB. This value comes from the Figure 3.2 on page 22. However, the simulation model used to obtain these results is rather high level so the results are bit optimistic. The author thinks that there are still room for improvements in the board design and control but the value of 30 dB of active cancellation is already very promising one.

Comparing the obtained cancellation values with other works presented in chapter 3 is done in the following Table 4.2. Stanford's first revision canceler cannot match the performance of this design. The main challenges in that design are the very delicate positions of antennas in order to provide isolation and the active chip, QHx220, used for cancellation. It seems to output significant side lobes which are undesired. 13 dB of active cancellation might not be enough to justify the use of active circuit providing cancellation.

On the other hand, Stanford's second revision canceler works very well and significant improvements are done with respect to revision I. They also use a circulator based approach the difference being in the cancellation tap structure. By using a total of 16 taps with external computer control they can reach a total analog domain cancellation of 72 dB over a 20 MHz bandwidth. The design works for higher bandwidths

Table 4.1. *Combined results from the measurement cases.*

Measurement case	**Intrinsic attenuation**	**Active cancellation**	**Total cancellation**
Circulator 20 MHz, Revision I canceler with revision II integrators, hybrid control	24 dB	33 dB	57 dB
Circulator 100 MHz, Revision I canceler with revision II integrators, hybrid control	22 dB	18 dB	40 dB
Relay antenna 20 MHz, Revision I canceler with revision I integrators, manual control	57 dB	22 dB	79 dB
Dual dipole antennas 20 MHz, Revision I canceler with revision II integrators, hybrid control	35 dB	27 dB	62 dB
Circulator 20 MHz, Revision II canceler with revision II integrators, self-adaptive control, see video	22 dB	24 dB to 34 dB	46 dB to 56 dB

Table 4.2. *Performance comparison of this canceler with other designs.*

Design and details	**Signal bandwidth**	**Active cancellation**	**Total cancellation**
This design in self-adaptive mode	20 MHz	24 dB to 34 dB	46 dB to 56 dB
Stanford revision I [2]	20 MHz	13 dB	46 dB
Stanford revision II [3]	20 MHz	-	72 dB
MIT Lincoln Laboratory [21]	≈80 MHz	≈18 dB	≈78 dB
Southeast University Nanjing [22]	20 MHz	30 dB	53 dB
Photonic Systems Incorporated [23, 24]	-	≈20 dB	≈70 dB

as well with lower total cancellations. Although our design provides less cancellation it can achieve the maximum of 56 dB by using only two taps in self-adaptive control. Also the exact amount of active cancellation is not specified which would be nice to know for comparison.

Measurements done by the Joseph G. McMichael and Kenneth E. Kolodziej from MIT Lincoln Laboratory are partly computer processed. They cut the recorded data to include reflections up to 1.75 m distance which obviously filters out some multipath components. The high intrinsic attenuation is due to long antenna separation.

Binqi Yang et al. from Southeast University Nanjing present similar results than in this paper using very similar approach. This canceler works well but the drawback is the only one cancellation tap. It means that the design works well provided that the frequency response of the cancellation tap and the SI channel are similar and the delay is matched very well. The adaptivity is claimed to be fast despite being blind search type algorithm. No demonstration is given though about the measured adaptivity and tracking.

Lastly the Photonic Systems Incorporated's approach is completely different than the others. They have focused on optical systems based circulator counterpart which can provide good amount of isolation over couple of decades of bandwidth. They demonstrate also total cancellation using digital only processing which is the value listed in the Table 4.2 [23]. So far their canceler is rather big being a size of a 19" rack mount device

4.6 Summary

The performance of the built cancelers was analyzed in this chapter. The overall RF parameters were good expect for couple of matching values. The author thinks this to be due to the very small couplers and the design of the co-planar waveguide transmission line.

The actual cancellation performance is in good order. Already the revision I canceler provided good cancellations and the updates and modifications of the revision II canceler improved especially the self-adaptive mode cancellation performance. The author values this the most as that would be the intended use for example in the mobile devices.

Comparing this work with respect to other works presented in academia it can be concluded that good cancellation values are obtained. Some of the designs provide better cancellations than in this design but they tend to be then more complex and/or larger physically.

5. CONCLUSIONS

In this thesis, an analog *radio frequency* (RF)-cancellation device based on a novel design was introduced, built and tested. RF-cancellation is crucial for in-band full-duplex operation where the main challenge is the cancellation of *self-interference* (SI). Cancellation is indispensable for the full-duplex operation and analog cancellation is required in order to protect the sensitive receiver circuitry and facilitate the requirements for digital cancellation.

The design is based on Intel's approach [11] and the key features are signal agnostic cancellation and self-adaptive control in fully analog design. The proposed and tested architecture can cancel whatever signal is fed to its input making the canceller very robust. The self-adaptive control is as important as the capability of cancellation itself. Without ability to track the changes of the SI-channel the usefulness of the canceller can be questioned.

The aim of this thesis and device is concept-proofing. That motivated the choices of components and optimizations to the design. The built device has two cancellation taps.

The results obtained from the built canceler conforms the thorough theoretical analysis presented in [11]. The most important measurement case, fully self-adaptive control, can provide an average of 30 dB cancellation varying between 24 dB to 34 dB depending on the echoes at the close proximity of the antenna. This result is obtained using a realistic *transmission* (TX) power of 20 dBm with a 20 MHz wide *long term evolution* (LTE) signal waveform. With manual or combined manual and self-adaptive control couple of more cancellation decibels could still be obtained. This means that the self-adaptive control is almost as good as it can get in the current design.

The cancellation for full-duplex operation is a joint operation and an overall system level capability of cancellation was tested with collaboration of Aalto University. Using a relay antenna designed in Aalto University [7], using this novel RF-canceller and post processing the data in digital domain using algorithms developed in Tampere University of Technology [19, 34] the system was able to completely cancel all the SI. The total cancellation in this case was almost 100 dB emphasizing the fact that despite enormous cancellation requirements by joint cancellation it can be done.

Comparing the results obtained with this canceler to other cancelers presented in academia or by companies shows that the results are very good. Few designs provide more cancellation being on the other hand more complex or using external control.

This thesis shows that analog RF-cancellation is both feasible and effective. It is indispensable and brings the full-duplex operation one step closer.

5.1 Future work

The current canceler, while working well, could be still improved for even more cancellation. It would be interesting to see the effect of third tap added to the design. That would by theory increase the cancellation for current test cases and make the canceller able to cancel even wider band signals. A smaller improvement would be still make a new revision of the board as although the design is revised many times on the computer screen one always finds slip(s) from the built device.

When aiming for practical design, the current design should be miniaturized, preferably in a form of a dedicated RF-chip. The current board is 10 cm $\times$ 12 cm and it is only for initial demonstration and prototyping purposes. At the same time various design parameters such as noise properties, insertion losses, maximum available cancellation power and power consumption need to weighed and make decision based on the most important parameter. It seems that unfortunately a trade-off must be made among the aforementioned parameters.

The current design is fully analog. The main drawback of it is the analog impairments especially in the control circuit. An interesting approach would be replace it, wholly or partly, with digital counterparts.

For any RF or antenna engineer in-band full-duplex presents many challenges waiting for optimizations. For example the antenna input matching needs to be fine-tuned for very high levels as the reflection from antenna contributes strongly to the SI. At the same time those optimizations are futile unless the circulator or electric balance network isolation is improved alongside. When targeting towards mobile devices, miniaturization is the key factor and alternatives for passive circulators must be found, unless operating at millimeter wave frequencies.

REFERENCES

[1] C. Shannon, "Communication in the presence of noise," *Proceedings of the IRE*, vol. 37, no. 1, pp. 10–21, Jan 1949.

[2] J. I. Choi, M. Jain, K. Srinivasan, P. Levis, and S. Katti, "Achieving single channel full duplex wireless communication," in *Proc. 16th Annual International Conference on Mobile Computing and Networking*, ser. MobiCom '10. New York, NY, USA: ACM, 2010, pp. 1–12.

[3] D. Bharadia, E. McMilin, and S. Katti, "Full duplex radios," in *Proc. SIGCOMM'13*, Hong Kong, China, August 2013.

[4] "Stanford Networked Systems Group: Full Duplex," Stanford University, Web site, Stanford, CA, [Visited 12.3.2015]. [Online]. Available: `http://snsg.stanford.edu/projects/full-duplex/`

[5] "About Us—Kumu Networks," Kumu Networks, Web site, Sunnyvale, CA, [Visited 7.4.2015]. [Online]. Available: `http://kumunetworks.com/about/`

[6] T. Huusari, Y.-S. Choi, P. Liikkanen, D. Korpi, S. Talwar, and M. Valkama, "Wideband self-adaptive rf cancellation circuit for full-duplex radio: Operating principle and measurements," in *Vehicular Technology Conference*, 2015, in press.

[7] M. Heino, D. Korpi, T. Huusari, E. Antonion-Rodríguez, S. Venkatasubramanian, T. Riihonen, L. Anttila, C. Icheln, K. Haneda, R. Wichman, and M. Valkama, "Recent advances in antenna design and interference cancellation algorithms for in-band full-duplex relays," *IEEE Communications magazine*, 2015, in press.

[8] J. Laskar, S. Chakraborty, A. Pham, and M. Tantzeris, *Advanced Integrated Communication Microsystems*, 1st ed. USA: Wiley-IEEE Press, 2007.

[9] *Oxford Dictionary of English*. Oxford, England: Oxford University Press, 2005.

[10] L. Hanzo, J. Blogh, and S. Ni, *3G, HSPA and FDD versus TDD Networking:Smart Antennas and Adaptive Modulation*. Chichester, England: Wiley-IEEE Press, 2008.

[11] Y.-S. Choi and H. Shirani-Mehr, "Simultaneous transmission and reception: Algorithm, design and system level performance," *IEEE Transactions on Wireless Communications*, vol. 12, no. 12, pp. 5992–6010, Dec. 2013.

[12] D. Korpi, S. Venkatasubramanian, T. Riihonen, L. Anttila, S. Otewa, C. Icheln, K. Haneda, S. Tretyakov, M. Valkama, and R. Wichman, "Advanced self-interference cancellation and multiantenna techniques for full-duplex radios,"

in *Signals, Systems and Computers, 2013 Asilomar Conference on*, Nov 2013, pp. 3–8.

[13] D. M. Pozar, *Microwave Engineering*, 4th ed. USA: Wiley, 2012.

[14] "Surface mount circulator/isolator," JQL Electronics, Catalogue, USA. [Online]. Available: http://www.jqlelectronics.com/Data%20&%20Catalog/Catalog/Surface_Mount_Isolator_Surface_Mount_Circulator.pdf

[15] W. L. Stutzmann and G. A. Thiele, *Antenna Theory and Design*, 3rd ed. USA: Wiley, 2013.

[16] "Agilent Time Domain Analysis Using a Network Analyzer," Agilent Technologies, Application Note 1287-12, USA, Jan. 2012. [Online]. Available: cp.literature.agilent.com/litweb/pdf/5989-5723EN.pdf

[17] "On Collective Frequencies for Licence-Exempt Radio Transmitters and Their Use," Ficora, Regulation, Helsinki, Finland, Dec. 2013. [Online]. Available: https://www.viestintavirasto.fi/attachments/Viestintavirasto15AF2013M_en.pdf

[18] "High-speed, analog-to-digital converter basics," Texas Instruments Corporation, Application report SLAA510, USA, 2011. [Online]. Available: www.ti.com/lit/an/slaa510/slaa510.pdf

[19] D. Korpi, T. Riihonen, V. Syrjala, L. Anttila, M. Valkama, and R. Wichman, "Full-duplex transceiver system calculations: Analysis of adc and linearity challenges," *Wireless Communications, IEEE Transactions on*, vol. 13, no. 7, pp. 3821–3836, July 2014.

[20] "Active isolation enhancer and interference canceller," Intersil Americas Incorporated, Data sheet, USA, 2009. [Online]. Available: https://www.intersil.com/content/dam/Intersil/documents/qhx2/qhx220.pdf

[21] J. McMichael and K. Kolodziej, "Optimal tuning of analog self-interference cancellers for full-duplex wireless communication," in *Communication, Control, and Computing (Allerton), 2012 50th Annual Allerton Conference on*, Oct 2012, pp. 246–251.

[22] B. Yang, Y. Dong, Z. Yu, and J. Zhou, "An rf self-interference cancellation circuit for the full-duplex wireless communications," in *Antennas Propagation (ISAP), 2013 Proceedings of the International Symposium on*, vol. 02, Oct 2013, pp. 1048–1051.

[23] C. Cox and E. Ackerman, "Demonstration of a single-aperture, full-duplex communication system," in *Radio and Wireless Symposium (RWS), 2013 IEEE*, Jan 2013, pp. 148–150.

[24] C. Cox and E. Ackerman, "Tiprx: A transmit-isolating photonic receiver," *Lightwave Technology, Journal of*, vol. 32, no. 20, pp. 3630–3636, Oct 2014.

[25] "Simultaneous Transmit and Receive (STAR)," Photonic Systems Incorporated, Web site, Billerica, MA, [Visited 12.3.2015]. [Online]. Available: http://www.photonicsinc.com/star_fm_demo.html

[26] "MAX2023," Maxim Integrated Products Incorporated, Data sheet revision 1, CA, USA, 2012. [Online]. Available: http://datasheets.maximintegrated.com/en/ds/MAX2023.pdf

[27] "HMC631LP3/631LP3E," Hittite Microwave Corporation, Data sheet revision 00.1007, MA, USA. [Online]. Available: https://www.hittite.com/content/documents/data_sheet/hmc631lp3.pdf

[28] Das, T., "Hittite's Vector Modulators," Hittite Microwave Corporation, Product Application Note, MA, USA, Jan. 2008. [Online]. Available: https://www.hittite.com/content/documents/application_notes/Vector%20Modulators.pdf

[29] "AD8341," Analog Devices Incorporated, Data sheet revision A, MA, USA, 2012. [Online]. Available: http://www.analog.com/static/imported-files/data_sheets/AD8341.pdf

[30] "MGA-638P8," Avago Technologies, Data sheet, USA, 2011. [Online]. Available: http://www.avagotech.com/docs/AV02-2993EN

[31] "AD835," Analog Devices Incorporated, Data sheet revision D, MA, USA, 2010. [Online]. Available: http://www.analog.com/static/imported-files/data_sheets/AD835.pdf

[32] "OPA734, OPA2734, OPA735, OPA2735," Texas Instruments Incorporated, Data sheet revision B, TX, USA, 2014. [Online]. Available: http://www.ti.com/general/docs/lit/getliterature.tsp?genericPartNumber=opa734&fileType=pdf

[33] R. R. Tummala, *Fundamentals of Microsystems Packaging*, 1st ed. USA: McGRAW-HILL, 2001.

[34] D. Korpi, "Analog Imperfections in Wireless Full-Duplex Transceivers," M. Sc. (eng.) thesis, Tampere University of Technology, Tampere, Finland, Feb. 2014.

APPENDIX 1: MESL CIRCULATOR MEASUREMENTS

Measured data of the MESL SG ser 104 circulator. Circulator was measured using HP-8722D *vector network analyzer* (VNA) and the three two-port .s2p-files were combined using Agilent ADS Touchstone Combiner -tool to create one .s3p-file.

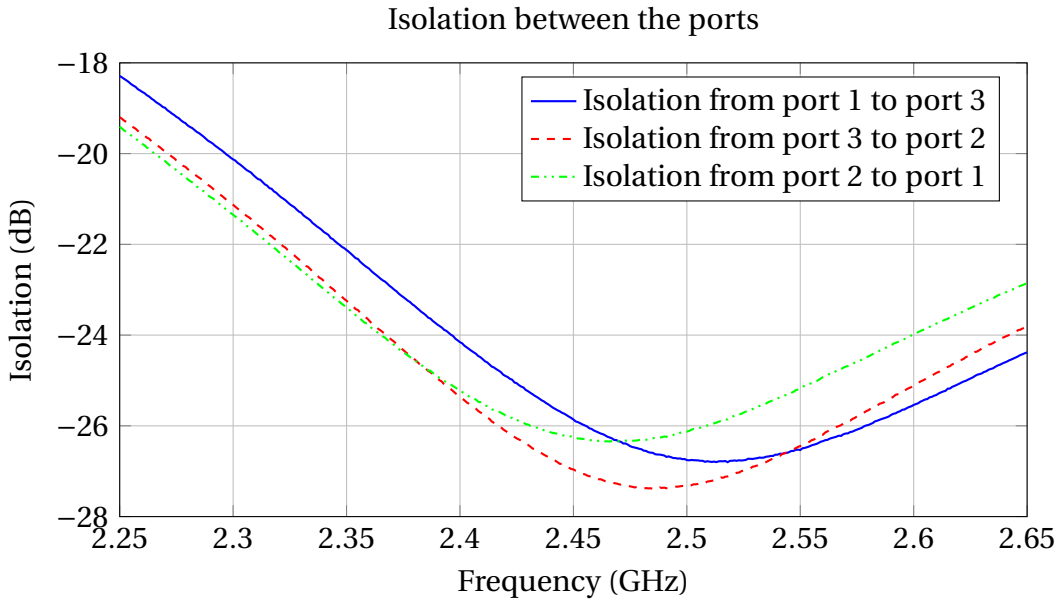

Figure A1.1

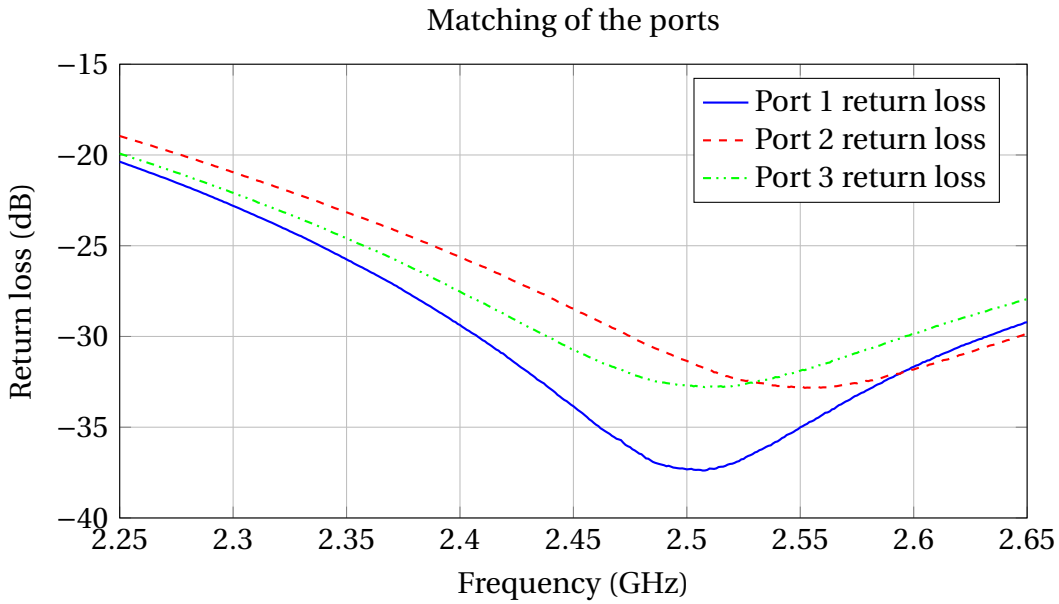

Figure A1.2

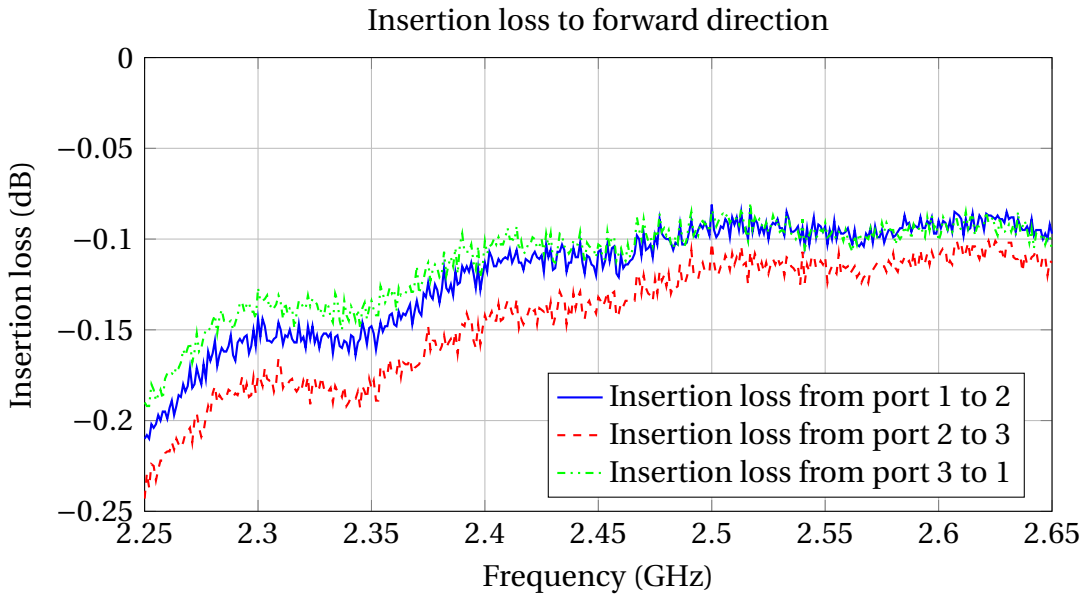
Insertion loss to forward direction
Insertion loss (dB)
0
−0.05
−0.1
−0.15
−0.2
−0.25
2.25
2.3
2.35
2.4
2.45
2.5
2.55
2.6
2.65
Frequency (GHz)
Insertion loss from port 1 to 2
Insertion loss from port 2 to 3
Insertion loss from port 3 to 1

Figure A1.3